

**Quantitative Estimate
of the
Air Quality Impacts
of
Methanol Fuel Use**

Prepared for the
California Air Resources Board
and the
South Coast Air Quality Management District
under ARB Agreement No. A6-048-32
by

Armistead Russell, Joel Harris,
Jana Milford and Debora St. Pierre
Department of Mechanical Engineering
Carnegie Mellon University
Pittsburgh, PA

April, 1989

Acknowledgements

Many people contributed to the successful and timely completion of this project. Thanks go to the California Air Resources Board (CARB) for both its funding of this work through agreement A6-048-32 and for the help of its staff. Particular thanks go to Manjit Ahuja, Steve Albu, Tom Cackette, Shewen Chen, Bart Croes, Don Drachand, John Holmes, Jack Paskind and Kit Wagner. Thanks go, too, to the staff of the South Coast Air Quality Management District (SCAQMD) for providing additional funding, critical data and their insights. In particular, Chung Liu, Alan Lloyd, and Paul Wuebben were valuable assets to this project. Mike McCormack of the California Energy Commission added valuable comments during the review of the draft report. The Methanol Task Force, now the Clean Fuels Working Group, including members from CARB, SCAQMD, and the California Energy Commission, provided direction on policy relevant issues.

Many members of the Carnegie Mellon and Pittsburgh Supercomputing Center communities added their expertise to the project, especially Greg McRae and Joel Welling. Mildred Gibb served to help produce the final document. Colleen Fischer, Damon Lipparelli, and Dan Stodolsky were instrumental in producing the computer graphics. At times during the execution of this project when it was imperative to get results "now" (when a calculation absolutely, positively, had to be done overnight), it was comforting to know that the CRAY XMP was available. Access to those facilities was made possible by CRAY Research and The Pittsburgh Supercomputing Center. A unique aspect of this project was the in-progress meetings attended by members of the effected parties - regulatory agencies, oil, gas and utility companies, motor vehicle manufacturers, academia, and consultants. We thank the participants of these meetings for their frank and open discussion of the study, so that concerns could be addressed directly, not after the fact.

As with any study of this type, there are bound to be errors or oversights, which are our responsibility. Feel free to communicate these with the authors. In writing the report, we have attempted to be objective, though personal views and interpretations may lead to certain statements and conclusions. When these are expressed, they are the sole responsibility of the authors. In fact:

The statements and conclusions in this report are those of the contractor and not necessarily those of the State Air Resources Board. The mention of commercial products, their source, or their use in connection with material reported herein is not to be construed as either an actual or implied endorsement of such products. In addition, they are not necessarily those of the South Coast Air Quality Management District.

Abstract

Methanol fuel use, in both mobile and stationary applications, has been proposed as a strategy to improve air quality in urban areas such as the South Coast Air Basin of California. It is viewed as a potential method to reduce, simultaneously, ozone, NO₂, particulate matter, benzene and other non-criteria pollutants such as peroxyacetyl nitrate and nitric acid. Currently the SoCAB, which encompasses Los Angeles, exceeds the federal and state limits for ozone, NO₂ and particulate matter. This provides the impetus to consider and test the effectiveness of methanol use to improve air quality. In order to assess, quantitatively, the impact that methanol fuel utilization could have in the SoCAB, a three-tiered, photochemical modeling study was designed and executed. The three tiers included chemical kinetics modeling, trajectory model analysis and, Eulerian, airshed modeling of ozone, NO_x, nitric acid, formaldehyde and peroxyacetyl nitrate. The design utilized the strengths of each model formulation to address the issues related to adopting policies for methanol utilization. Particulate matter response to methanol use was calculated from results of photochemical and non-photochemical modeling. Formaldehyde, methanol and benzene buildup under stagnation conditions, and the response to methanol use, was determined using linear modeling. These models were used to study the air quality benefits of methanol use in motor vehicles and stationary sources for the years 2000 and 2010.

One of the most cited potential benefits of switching to methanol fuel is to reduce ozone which is a severe problem in the SoCAB. Over ninety other urban areas also experience ozone levels in excess of the national standard. Chemical kinetics modeling and sensitivity analysis showed that methanol emissions do not add greatly to the formation of ozone, even over multiday episodes. This conclusion was reinforced by trajectory and airshed modeling that showed that the methanol component of the exhaust of methanol fueled vehicles led to little change in the ozone predicted to be formed. A three day period, that was conducive to producing high ozone concentrations, was simulated using the air quality models. The buildup of methanol over the multiday smog episode did not eliminate the ozone reduction potential of utilizing methanol as a motor vehicle fuel. Ozone reductions of up to 17% were predicted for utilizing M100 fueled vehicles. This was 77% of the reduction of removing motor vehicle source emissions completely. The reduction was limited by the relatively small fraction of the total ROG forecast to be attributable to motor vehicles in the year 2000.

Formaldehyde emissions, and the gasoline fraction of methanol fuel blends, proved to be significant contributors to ozone formation. Use of M85, or increased emissions of formaldehyde from motor vehicles (55 mg mi⁻¹ of HCHO vs. 15-18 mg mi⁻¹ as modeled in the base case) led to only half the improvement in the predicted ozone concentrations and exposures. Recent tests, however, indicate that the exhaust and evaporative emissions from M85 may be less reactive than modeled, which would increase the improvements to be expected and decrease the apparent difference between M85 and M100 fuel use.

A concern before this study was that the increased direct emissions of formaldehyde from methanol fueled vehicles would lead to excessive HCHO levels. Calculations by the photochemical models showed that formaldehyde levels during smog episodes should not increase greatly, and may in fact decrease. The reduction in HCHO levels is a result of the low reactivity of methanol leading to lower atmospheric production, offsetting the increased emissions. Formaldehyde exposures, based on methanol fueled light duty vehicles emitting between 15 and 18 mg mi⁻¹ (in use), were 17% less and 13% more than the corresponding base cases for year 2000 and 2010 calculations, respectively.

Concentrations of other pollutants would also decrease if methanol was used. Particulate matter concentrations would decrease because methanol fueled vehicles emit less aerosol carbon than the corresponding conventionally fueled counterparts, especially diesels. Also, emissions of gas phase precursors to aerosol formation, and atmospheric production of particulate matter, is reduced. Particulate matter levels could be reduced up to 19%, based on the annual average at Rubidoux. In particular, aerosol carbon and aerosol nitrate levels would be reduced. Areas heavily impacted by these components would benefit the greatest. Predicted nitric acid, NO_2 and peroxyacetyl nitrate (PAN) were reduced from switching to methanol. Methanol is not a precursor to PAN, and reductions of up to 22% were predicted. Exposures to nitric acid and NO_2 concentrations were predicted to decrease about 28%.

Ambient methanol levels would increase to about 1 ppm under extreme stagnation conditions. HCHO concentrations could approach 90 ppb. This is an order of magnitude less than the OSHA standard. Motor vehicles, powered by conventional fuels, are projected to be the major contributors to ambient benzene in the SoCAB. Switching to methanol would decrease ambient levels of benzene, a carcinogen. Thus, methanol could be used effectively to improve many aspects of air quality in the Los Angeles area.

Table of Contents

Acknowledgements	i
Abstract	iii
List of Tables	ix
List of Figures	xi
List of Frequently Used Abbreviations	xiv
1.0 Introduction	1
1.1 Methanol as a Clean Alternative Fuel	1
1.2 Objective of this Study	3
1.3 Qualitative Description of Expected Air Quality Impacts	3
1.4 Methodology of this Study	9
1.5 Outside Project Participation	10
1.6 Previous Studies: Results and Limitations	10
1.6.1 Mathematical Modeling Studies	11
1.6.2 Experimental Studies	12
1.7 Organization of this Report	13
2.0 Chemical Mechanism Evaluation	15
2.1 Introduction	15
2.2 Chemical Mechanism	15
2.3 Mechanism Evaluation	16
2.3.1 SAPRC Smog Chamber Experiments	19
2.3.2 Test Results	20
2.3.2.1 ITC Test Results	20
2.3.2.2 OTC Test Results	27
2.3.3 Alternative Chemical Mechanisms	27
2.4 Limitations of Smog Chamber Results for Evaluating Methanol Strategy Effectiveness	33
2.5 Conclusion	34
3.0 Sensitivity Analysis of the Chemical Mechanism and Ozone Production to Methanol and Formaldehyde	35
3.1 Simulation and Sensitivity Analysis Methods and Conditions	35
3.1.1 The Caltech Mechanism	35
3.1.2 The SAPRC/ERT Mechanism	36
3.1.3 Simulation Conditions	36
3.1.4 Sensitivity Analysis Methodology	38
3.2 Simulation and Sensitivity Analysis Results	39
3.3 Ozone Sensitivity to Initial Conditions and Emissions	42
3.4 Summary of Sensitivity Results	46
4.0 Photochemical Air Quality Model Inputs	47
4.1 Introduction	47
4.2 Selection of the Modeling Period	48
4.3 Modeling Region	48
4.4 Meteorological Fields and Air Quality Data	50
4.5 Selection of Future Modeling Years	50
4.6 Base Emission Inventories	50
4.7 Creation of Alternate Emissions Databases	53
4.7.1 Inventory De-aggregation and Construction	53
4.7.2 On-Road Mobile Sources Database	55

4.7.3	Altering Off-Road Mobile Source Databases	57
4.7.4	Altering Petroleum Refinery Databases	57
4.7.5	Altering Utility Boiler and Power Plant Databases	58
4.7.6	Altering Petroleum Retail Marketing Databases	58
4.7.7	Stationary Internal Combustion Engines	59
4.8	Summary	59
	Appendix 4.A	61
	Appendix 4.A1	63
	Appendix 4.B	64
	Appendix 4.C	66
	Appendix 4.D	67
	Appendix 4.E	68
	Appendix 4.F	71
5.0	Trajectory Modeling of Ozone, PAN and Formaldehyde	72
5.1	Introduction	72
5.2	Trajectory Model Formulation	72
5.3	Description of Trajectory Paths	73
5.4	Trajectory Scenarios	76
5.5	Results	77
5.5.1	Ozone Sensitivity to Methanol Fuel Use Levels	83
5.5.2	Sensitivity to Formaldehyde Exhaust Fraction	89
5.5.3	Ozone Sensitivity to Varying Deterioration Rates	89
5.5.4	Use of Advanced Conventional and Methanol Fueled Vehicles	90
5.5.5	Role of Emission Timing	90
5.5.6	Response of Formaldehyde and PAN to Emission Changes	90
5.6	Summary of Trajectory Modeling	97
6.0	Airshed Modeling of Ozone, PAN, and Formaldehyde	99
6.1	Introduction	99
6.2	Airshed Model Description	99
6.3	Model Performance Evaluation	101
6.4	Description of Airshed Model Calculations for Future Years	105
6.4.1	Base Case Calculations for the Years 2000 and 2010	110
6.4.2	Diagnostic Calculations	110
6.4.3	Descriptions of Control Calculations	115
6.4.3.1	Year 2000 Calculations	115
6.4.3.2	Year 2010 Calculations	117
6.5	Effect of Fuel Conversion	118
6.5.1	Measures of Pollutants Levels	118
6.5.2	Baseline Air Quality Predictions	140
6.5.3	Diagnostic Calculations	141
6.5.4	Methanol and Conventional Fuel Scenario Results	143
6.5.4.1	Control of Conventionally Fueled Vehicles	144
6.5.4.2	Effectiveness of Fuel Types	144
6.5.4.3	Advanced Technology Vehicles	145
6.5.4.4	Formaldehyde Exhaust Fraction	146
6.5.4.5	Partial Penetration of Methanol Fueled Vehicles	147
6.5.4.6	Stationary Source of Methanol	147
6.5.4.7	Clean Initial and Boundary Condition Control Simulations	147

6.6 Summary and Conclusions	148
7.0 Aerosol Modeling of the Impact of Methanol Fuel Use	150
7.1 Introduction	150
7.2 Primary Carbon Aerosols	151
7.2.1 Fine Carbon and Fine Elemental Carbon	151
7.2.2 Source Receptor Analysis of Carbon Aerosol Concentrations	152
7.2.3 Source Emissions of Fine Carbon	153
7.2.4 Determining Fine Carbon Concentrations	154
7.2.5 Results	154
7.2.5.1 Areawide Fine Carbon Levels	154
7.2.5.2 Fine Carbon Levels at Specific Locations	158
7.2.6 Summary of Carbon Particulate Modeling	170
7.3 Aerosol Nitrates	170
7.3.1 Aerosol Nitrate-Emission Relationships	170
7.3.2 Results and Discussion	171
7.3.3 Summary of Aerosol Nitrate Results	173
7.4 Particulate Sulfate	173
7.4.1 Sources of Sulfur in the SoCAB	173
7.4.2 Aerosol Sulfate Concentrations	175
7.4.3 Calculation Methodology	175
7.4.4 Summary of Impact on Sulfate	175
7.5 Organic Aerosols	175
7.5.1 Formation of Organic Aerosols	176
7.5.1.1 Cyclic Olefins and Diolefins	176
7.5.1.2 Aromatic Hydrocarbons	178
7.5.2 Results and Discussion	179
7.5.3 Summary of Secondary Organic Aerosol Modeling	183
7.6 Future PM ₁₀ Levels	183
7.6.1 Description of AQMP PM ₁₀ Modeling Methodology	183
7.6.2 Integration of PM ₁₀ Modeling of Methanol Utilization	185
7.6.3 Discussion of PM ₁₀ Effects	190
7.6.4 Summary of PM ₁₀ Effects	190
7.7 Visibility	190
7.8 Summary of Aerosol and Visibility Modeling	195
8.0 Wintertime Formaldehyde and Methanol Levels Under Low Ventilation, and the Impact on Benzene	199
8.1 Introduction	199
8.2 Formaldehyde	199
8.2.1 Calculation Methodology	200
8.2.2 Discussion of Formaldehyde Buildup	203
8.2.3 Summary of Peak, Wintertime Formaldehyde Levels	203
8.3 Peak Methanol Concentrations	204
8.3.1 Expected Ambient Methanol Concentrations	204
8.3.2 Discussion	205
8.4 Ambient Benzene Concentrations	205
8.5 Summary of Methanol, Formaldehyde and Benzene Concentrations Resulting from MFV Use	206
Appendix 8.A	207

9.0 Recommendations for Future Work	208
9.1 Exhaust Composition of M85 and M100 Fuel	208
9.2 Modeling of Other Episodes	209
9.3 Use of a Different Chemical Mechanism	209
9.4 Other Alternative Fuels	210
9.5 Impact of Methanol Downwind of Los Angeles	210
9.6 Incorporating the Results of the Adoption of the Air Quality Management Plan	210
9.7 Impacts on Aqueous Phase Chemistry	211
9.8 Summary of Recommendations	211
10.0 Summary of the Air Quality Effects of Methanol Utilization	212
10.1 Summary of Issues and Related Conclusions	212
10.1.1 Multiday Build-Up of Methanol Decreasing Effectiveness	212
10.1.2 Will Ambient Formaldehyde Levels Increase?	212
10.1.3 Will Methanol Levels Build Up to Unhealthful Levels?	213
10.1.4 How Will Methanol Use Affect Concentrations of Pollutants Other Than Ozone, HCHO and Methanol?	213
10.2 Summary of Expected Improvement in Air Quality From Utilizing Methanol	213
10.2.1 Potential Benefits of Methanol Fueled Vehicle Fleets Compared to Conventionally Fueled Vehicles	214
10.2.2 Effectiveness of Fuel Types	214
10.2.3 Exhaust Formaldehyde Content	215
10.2.4 Low Emitting Methanol and Conventionally Fueled Vehicle Fleets	215
10.2.5 Stationary Use of Methanol Fuel	215
10.2.6 Example of Use of Results for Intermediate Cases	216
10.3 Impact on Particulate Matter and Visibility	216
10.4 Benzene Reductions	217
10.5 Future Studies	217
10.6 Conclusion	217
References	219

List of Tables

Chapter 1

Table 1.1	Issues Concerning Methanol Impacts on Air Quality
Table 1.2	Three-Tiered Modeling Structure

Chapter 2

Table 2.1	Chemical Mechanism Reactions
Table 2.2	ROG/NO _x Ratios
Table 2.3	ITC Predicted and Observed Peak Ozone Concentrations
Table 2.4	ITC 872 Data
Table 2.5	OTC Predicted and Observed Peak Ozone Concentrations

Chapter 3

Table 3.1	Initial Conditions used in Kinetic Simulations
Table 3.2	Predicted Ozone Concentrations
Table 3.3	Concentrations of HCHO, HNO ₃ and PAN

Chapter 4

Table 4.1	Summary of 1982 Emissions
Table 4.2	Summary of Year 2000 Emissions
Table 4.3	Summary of 2010 Emissions

Chapter 5

Table 5.1	List of Emissions Scenarios
Table 5.2	Ozone, Formaldehyde, and PAN in the San Bernardino Trajectory
Table 5.3	Ozone, Formaldehyde, and PAN in the Pasadena Trajectory
Table 5.4	Ozone, Formaldehyde, and PAN in the Norco Trajectory

Chapter 6

Table 6.1	Summary of Model Performance Statistics
Table 6.2	Airshed Model Scenarios
Table 6.3	Emissions Totals
Table 6.4	Ozone Concentrations and Exposures in the Year 2000
Table 6.5	Pollutant Concentrations and Exposures in the Year 2000
Table 6.6	Ozone Concentrations and Exposures in the Year 2000, Day 2
Table 6.7	Pollutant Concentrations and Exposures in the Year 2000, Day 2
Table 6.8	Basin wide Ozone Concentrations and Area Exposures, Year 2000
Table 6.9	Ozone Concentrations and Exposures in the Year 2010
Table 6.10	Pollutant Concentrations and Exposures in the Year 2010
Table 6.11	Ozone Concentrations and Exposures in the Year 2010, Day 2
Table 6.12	Pollutant Concentrations and Exposures in the Year 2010, Day 2
Table 6.13	Basin wide Ozone Concentrations and Area Exposures, Year 2010
Table 6.14	Comparison of BASE1 Results with Scenario 2000x

Chapter 7

Table 7.1	Total and Elemental Carbon Emissions for the Modeling Region
Table 7.2	Concentration and Sources of Fine and Elemental Carbon at Los Angeles and Lennox
Table 7.3	Projected, Year 2000, Nitrate emissions, Concentrations, and Exposures
Table 7.4	SO _x Emission Sources and Their Contribution to Particulate Sulfate
Table 7.5	Vapor Pressures of Reaction Products of Olefinic Precursors
Table 7.6	Dicarboxylic Acid and Dinitrocresol Concentrations for Selected Scenarios
Table 7.7	Source Contributions to PM ₁₀ at Rubidoux in 1986
Table 7.8	Source Contributions to Annual Average Secondary Sulfate and Nitrate at Rubidoux in 1986
Table 7.9	Predicted, Year 2000, Source Contributions to Annual Average Aerosol Nitrate (PM ₁₀) at Rubidoux
Table 7.10	Projected Source Contributions to Annual Average Sulfate (PM ₁₀) Levels at Rubidoux
Table 7.11	Predicted Year 2000 Annual Average PM ₁₀ at Rubidoux
Table 7.12	Peak, 24-hr average PM ₁₀ at Rubidoux
Table 7.13	Predicted Visibility Extinction at Rubidoux

Chapter 8

Table 8.1	Annual Maximum CO Concentrations in the South Coast Air Basin, 1979-1987
-----------	---

List of Figures

Chapter 1

- Figure 1.1 ROG and NO_x Emissions in the Year 2000
 Figure 1.2 Reactivity Weighted Emissions of CFVs vs. MFVs
 Figure 1.3 Model of Air Quality Model of the Atmosphere

Chapter 2

- Figure 2.1 Peak ITC Ozone Concentrations
 Figure 2.2 Peak ITC Ozone Concentrations vs. NO_x/ROG Ratio
 Figure 2.3 Ozone, PAN, and HCHO Concentrations from ITC
 872
 Figure 2.4 Peak OTC Ozone Concentrations
 Figure 2.5 Ozone Concentrations for OTC Runs
 Figure 2.6 PAN Concentrations for OTC Runs
 Figure 2.7 HCHO Concentrations for OTC Runs
 Figure 2.8 Pollutant Species Concentrations for OTC Run 231
 Figure 2.9 Pollutant Species Concentrations for OTC Run 231

Chapter 3

- Figure 3.1 Predicted ozone as a function of time using the Caltech
 and SAPRC/ERT mechanisms
 Figure 3.2 Semi-normalized sensitivity of ozone formation to initial
 conditions
 Figure 3.3 Semi-normalized sensitivity of ozone formation to
 emissions

Chapter 4

- Figure 4.1 Methodology to disaggregate, manipulate, and
 reconstruct the emissions inventory

Chapter 5

- Figure 5.1 Graphical Representation of the Lagrangian
 Trajectory Model
 Figure 5.2 Map of Trajectory Paths in the SoCAB
 Figure 5.3 Ozone reduction as a percentage of M100 MFV
 penetration into the vehicle fleet
 Figure 5.4 Ozone reduction as a percentage of M85 MFV
 penetration into the vehicle fleet
 Figure 5.5 Ozone sensitivity to the Formaldehyde Fraction of M100
 MFV Emissions
 Figure 5.6 Ozone sensitivity to the Formaldehyde Fraction of M85
 MFV Emissions

Figure 5.7	Ozone response to Changes in Emissions Deterioration Rates
Figure 5.8	Effect of changing vehicle emission timing
Figure 5.9	Predicted ozone for advanced CFV and MFV vehicle fleets
Figure 5.10	Formaldehyde Fraction of MFV Emissions Effect on Ambient Formaldehyde Levels
Figure 5.11	Formaldehyde Fraction of M85 MFV Emissions Effect on Ambient Formaldehyde Levels
Figure 5.12	Percentage of MFV Penetration into the Vehicle Fleet, Effect on Ambient Formaldehyde
Figure 5.13	Percentage of MFV Penetration into the Vehicle Fleet, Effect on Ambient PAN

Chapter 6

Figure 6.1	Enlarged Modeling Region
Figure 6.2	Predicted and Observed Ozone and PAN
Figure 6.3	Predicted and Observed Oxidized Nitrogen Compounds
Figure 6.4	Emissions of Pollutant by Scenarios
Figure 6.5	Spatial Distribution of Ozone on Third Day, 1 PM , Year 2000, (BASE1A, BASE1, LO IC, 1982)
Figure 6.6	Spatial Distribution of Ozone on Third Day, 1 PM Year 2000, (NO EM, NO ROG, NO ROG/LO IC, NO EM/LO IC)
Figure 6.7	Spatial Distribution of Ozone on Third Day, 1 PM Year 2000, (NO MOBILE, BASE-ROG, BASE-NOX)
Figure 6.8	Spatial Distribution of Ozone on Third Day, 1 PM Year 2000, (ADV CONV, ADV METH, STD M100, FULL METH)
Figure 6.9	Spatial Distribution of Ozone on Third Day, 1 PM Year 2000, (METH 50, STD M85, HIGH FORM, ADV METH/NO ROG)
Figure 6.10	Spatial Distribution of Ozone on Third Day, 1 PM Year 2010, (BASE 2010, CLEAN BC 2010, LO BC/LO IC 2010, NO ROG/LO IC 2010)
Figure 6.11	Spatial Distribution of Ozone on Third Day, 1 PM Year 2010, (ADV METH 2010, ADV CONV 2010, NO MOBILE 2010, NO MOBILE ROG 2010)
Figure 6.12	Spatial Distribution of Ozone on Third Day, 1 PM Year 2010, (STD M85 2010, STD M100 2010, ADV LMD 2010, ADV LMD/NO ROG 2010)
Figure 6.12	Spatial Distribution of Ozone on Third Day, 1 PM Year 2010, (LO IC 2010, ADV CONV/LO IC 2010, ADV METH/LO IC 2010, STD M85/LO IC 2010)

Chapter 7

- Figure 7.1 Total Carbon Emissions in 1982 and Year 2000 Scenarios
- Figure 7.2 Elemental Carbon Emissions in 1982 and Year 2000 Scenarios
- Figure 7.3 Concentrations and Sources of Fine Total Carbon at Los Angeles, September Period
- Figure 7.4 Concentrations and Sources of Fine Elemental Carbon at Los Angeles, September Period
- Figure 7.5 Concentrations and Sources of Fine Total Carbon at Los Angeles, December Period
- Figure 7.6 Concentrations and Sources of Fine Elemental Carbon at Los Angeles, December Period
- Figure 7.7 Concentrations and Sources of Fine Total Carbon at Lennox, September Period
- Figure 7.8 Concentrations and Sources of Fine Elemental Carbon at Lennox, September Period
- Figure 7.9 Concentrations and Sources of Fine Total Carbon at Lennox, December Period
- Figure 7.10 Concentrations and Sources of Fine Elemental Carbon at Lennox, December Period
- Figure 7.11 Average of Reduction Sensitivities for Dicarboxylic Acids and Dinitrocresols
- Figure 7.12 Source Contributions to Annual Average PM_{10} at Rubidoux in the Year 2000
- Figure 7.13 Source Contributions to Peak, 24-hr average PM_{10} at Rubidoux in the Year 2000
- Figure 7.14 Source Contributions to Annual Average Visibility Extinction at Rubidoux in the Year 2000

List of Frequently Used Abbreviations

ACGIH	American Conference of Governmental Industrial Hygienists
AQMP	Air Quality Management Plan for the SoCAB (either the 1982 or the 1988 draft)
CARB	California Air Resources Board
CFV	Conventionally Fueled Vehicle
CH ₄ O	Chemical symbol for methanol
CIT	California Institute of Technology and/or Carnegie Institute of Technology
CMU	Carnegie Mellon University
CYC	Cycloalkenes and diolefins
DI-ACID	Dicarboxylic acids
DNC	Dinitrocresol
EPA	Environmental Protection Agency
EQL	Environmental Quality Labs
ERT	Environmental Research and Technology
FFV	Flexible Fuel Vehicle
FTP	Federal Test Procedure
HCHO	Chemical symbol for formaldehyde
HDV	Heavy Duty Vehicle
HEI	Health Effects Institute
ITC	Indoor Teflon Chamber
JPL	Jet Propulsion Labs
LDV	Light Duty Vehicle
M100	Fuel compound of nearly 100% methanol fuel
M85	Fuel compound of 85% methanol, 15% other organics
MFV	Methanol Fueled Vehicle
MTF	Methanol Task Force
NAAQS	National Ambient Air Quality Standards
NIOSH	National Institute of Occupational Safety and Health
NMHC	Non-methane, non-methanol hydrocarbons (also known as NMOG)
NMOG	Non-methane, non-methanol organic gases
OSHA	Occupational Safety and Health Administration
OTC	Outdoor Teflon Chamber
PAN	Peroxyacetyl nitrate
PAH	Polycyclic Aromatic Hydrocarbons
PM ₁₀	Particulate matter less than 10 mms in diameter
RDA	Reaction-Diffusion-Advection (equation)
RVP	Reid vapor pressure
ROG	Reactive Organic Gases
SAPRC	Statewide Air Pollution Research Center (University of California, Riverside)
SCAG	Southern California Association of Governments
SCAQMD	South Coast Air Quality Management District
SCAQS	Southern California Air Quality Study
SoCAB	South Coast Air Basin of California, which includes Los Angeles and surrounding regions
THC	Total Hydrocarbons (also known as TOG)
TOC	Total organic carbon
TOG	Total organic gases
•	Radical (A highly reactive, unstable molecule)

1.0 Introduction

1.1 Methanol as a Clean Alternative Fuel

Methanol is considered to be one of the most promising "clean" alternative fuels, replacing gasoline and diesel oil in internal combustion engines. Methanol is cited as having the potential to substantially reduce the pollution attributable to motor vehicle internal combustion engines, and can be used in conjunction with conventional fuels in stationary sources, such as utility boilers and refinery heaters, to reduce emissions. It is also believed that the development of an alternative fuel such as methanol would reduce our dependence on foreign oil. However, conversion from petroleum-derived fuels would, of course, have a tremendous effect on industry, and the environmental benefits must be weighed against the possible economic costs of adopting a strategy involving methanol.

Before adopting a strategy with the economic and environmental consequences as would be experienced by large scale utilization of methanol, it is necessary to *a priori* identify and quantify both the likely benefits and problems. The information should be developed in a fashion that will provide a solid, scientifically defensible foundation to support policy decisions. This study has been designed to be part of that foundation by developing quantitative estimates of the air quality impact of adopting strategies involving extensive methanol use in the South Coast Air Basin (SoCAB) of California. The SoCAB, which includes Los Angeles and the surrounding area, is regarded as having the most severe photochemical smog problem in the United States. A relatively large fraction of the pollutant causing emissions are from mobile sources. This makes the SoCAB a good candidate for testing the role methanol can play in improving air quality and for identifying the important issues involved in methanol control strategies. This study is oriented towards the critical issues, addressing questions left unanswered by previous studies, and answering questions more recently identified.

One example of the issues addressed is the formaldehyde content of methanol fueled vehicles (MFV) exhaust. The percent of formaldehyde in MFV exhaust is believed to be a critical parameter in determining environmental impacts. For this reason, the California Air Resources Board (CARB) has considered adopting a separate standard for formaldehyde emissions. Specific calculations were conducted to provide guidance on the air quality response to varying levels of formaldehyde emissions. Calculations conducted as part of this project estimate the potential reductions in ozone, nitrogen dioxide (NO₂), peroxyacetyl nitrate (PAN), and fine particulate matter (PM₁₀), the buildup of formaldehyde and methanol under severe conditions, and the impact on acid deposition. A list of issues, and a brief synopsis of the findings, are given in Table 1.1. Support for the conclusions drawn are found in the chapters referenced.

Acceptance of a methanol strategy, or any alternative fuel, will depend on the choice of initial applications, and the success of methanol in those early applications. This study provides key information to identify which applications would lead to air quality improvements from conversion to methanol. Calculations show the air quality benefits of converting light duty automobiles, heavy duty diesel vehicles, and stationary sources can be compared given the results of this study.

Methanol has the potential to reduce concentrations of ozone, nitrogen dioxide, and particulate matter, benzene, PAN and nitric acid, and can improve visibility and reduce acid deposition. As will be seen in this study, its use may also lower formaldehyde levels. Currently, the South Coast Air Basin exceeds national and state standards for each of the pollutants mentioned. Ozone levels of over three times the National Ambient Air Quality Standard (NAAQS) of 0.12 ppm, or four times the State standard of 0.09 ppm, are

Table 1.1 Issues Concerning Methanol Impacts on Air Quality

<u>Issue</u>	<u>Brief Summary of Findings</u>	<u>Reference Chapters</u>
1) Multiday buildup of methanol decreasing effectiveness for reducing ozone	Contrary to analysis of experimental findings, buildup, and multiday residence of methanol emissions do not greatly decrease the ozone reduction from switching to methanol. The experimental findings are explained by the apparatus and test procedures.	2, 3, 5, 6
2) Increase in ambient formaldehyde	Ambient HCHO will not increase significantly from switching to MFVs, and may, in fact, decrease. The increase in direct emissions is offset by a decrease in gas phase HCHO production. Wintertime levels should remain within recommended range.	5, 6, 7
3) Formaldehyde content of MFV exhaust	Increasing exhaust formaldehyde from 15-18 mg mi ⁻¹ to 55 mg mi ⁻¹ decreased ozone reduction by ~50%. Ambient formaldehyde exposure increased 38%, though remained much less than the suggested standard.	6
4) Will methanol increase to unhealthful levels?	Modeling in this study and literature review indicate that direct exposure to ambient methanol will not be a problem.	8
5) To what extent will methanol utilization impact other pollutants?	NO ₂ , HNO ₃ and PAN concentrations and exposures expected to decrease, on average, about 25 - 30%. Particulate matter could decrease up to 19%, on an annual average, and peak 24-hr levels could decrease up to 35%.	7
6) How effective would methanol use be for reducing ozone?	Predicted ozone reductions ranged up to 17%. This was 77% as effective as totally removing mobile source emissions. The extent of the reduction is limited by the fraction of ROG due to on-road motor vehicles.	5, 6
7) What future studies are needed to provide the necessary data for more accurate models?	The major uncertainty encountered in this project was the dearth of data on MFV emissions. Estimates of future emissions are even less well established. Projects to rectify this need are a first priority. Other projects include modeling other episodes and looking at the aqueous phase reactions.	4, 9

recorded during severe episodes. In a recent study (Soloman et al., 1988), fine particulate matter (PM₁₀) concentrations of almost twice the national 24 hr standard of 150 $\mu\text{g m}^{-3}$ and six times the state standard of 50 $\mu\text{g m}^{-3}$, were measured in the eastern portion of the SoCAB. Nitrogen dioxide (NO₂) concentrations occur in excess of the national and state standards of 0.0536 (annual average) and 0.25 ppm (1-hr. average), respectively. Benzene, a carcinogen, is directly emitted by conventionally fueled vehicles, and switching to methanol would reduce ambient concentrations. No lower bound has been set on what is considered to be an acceptable ambient level of benzene.

Studies have found that no control strategy which relies strictly on current control techniques appears capable of reducing ozone concentrations to meet the standards, and partial reductions will come only at a great cost (SCAQMD and SCAG; 1982, 1988). The need to concurrently reduce benzene, particulate matter and NO₂ concentrations adds further complexity to the problem. In light of the severe problem experienced in the SoCAB and the potential for methanol to improve each aspect discussed, serious consideration must be given to a strategy involving methanol as an alternative fuel.

1.2 Objective of this Study

The goal of this study is to quantify the air quality impacts resulting from the use of methanol fuel in a variety of applications within the SoCAB. This is done by using a series of advanced air quality models to determine air quality in the SoCAB as a function of emissions. As listed in Table 1.1, issues addressed deal with the impact of methanol fuel utilization on air quality. In particular, the models are used to predict how ambient concentrations of ozone, particulate matter, formaldehyde, nitric acid, benzene, methanol, and peroxyacetyl nitrate would be expected to change if there was a trend towards widespread utilization of methanol. Figure 1.1 shows the general structure of the air quality models employed. These models describe, mathematically, the important processes that affect the evolution of pollutants in the atmosphere. Inputs to the model are the emissions into the atmosphere and the prevailing meteorology. The output is the predicted air quality. By exercising these models over a range of emissions inputs, simulating the adoption of different methanol fuel use strategies, it is possible to determine the complex source-air quality relationships. Different models are used in this study to take advantage of each models' strengths.

Uncertainty is inherent in any modeling study, especially when applied to forecasting the probable effects of a relatively new strategy years in the future as is being done here. A second objective of this study is to identify the major areas of uncertainty, and to quantify their effects. A three tiered modeling approach has been adopted to do this most effectively. A list of the models employed, along with their strengths and limitations, is given in Table 1.2. Chemical kinetics modeling, trajectory model analysis, and airshed modeling are all used to develop the view of the impact of methanol fuel use on air quality.

1.3 Qualitative Assessment of Expected Air Quality Impacts

Much of the attention on methanol has focused on its ability to reduce ozone. This is true not only in the SoCAB, but nationally. Over 68 urban areas are out of compliance with the ozone standard. The SoCAB, however, experiences the highest ozone levels nationally. Ozone (O₃) is an oxidant that has adverse effects on the human respiratory system, agriculture, and materials (Lioy et al. 1985, Bresnitz and Rest, 1988). Recent studies suggest that the 0.12 ppm standard may leave little or no margin of safety, and tightening the standard has been suggested (Lioy et al. 1985, Lippmann et al. 1983). California, in response to the studies, has lowered the standard to 0.09 ppm.

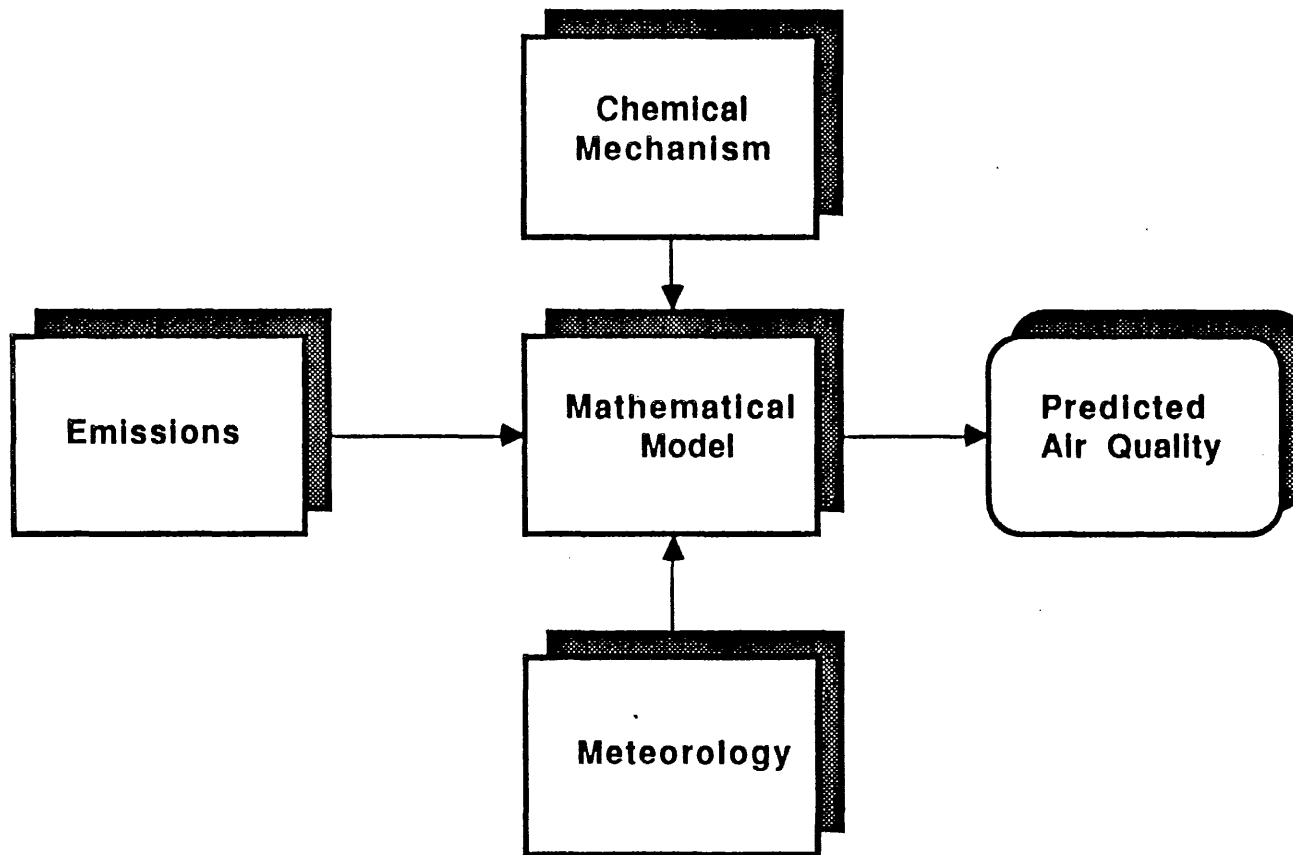
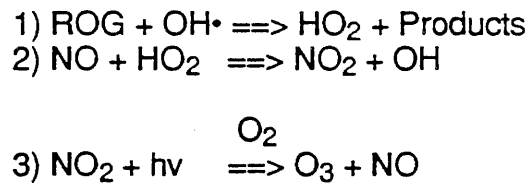


Figure 1.1 Components of an air quality modeling study. An air quality model, by accurately describing atmospheric chemistry and meteorology, can be used to develop emissions - air quality relationships.

**Three-Tiered Modeling Structure:
Strengths, Weaknesses and Uses of Each Model**

	<u>Strengths</u>	<u>Weaknesses</u>	<u>Uses</u>
Tier 1: Chemical Kinetics Modelling	<p>Fast. Allows for extensive mechanism testing.</p> <p>Good for identifying chemical pathways.</p> <p>Output can be compared to smog chamber mechanisms.</p> <p>Isolates chemistry from atmospheric dynamics</p>	<p>Does not describe atmospheric dynamics of fresh emissions.</p>	<p>Testing chemical mechanisms.</p> <p>Sensitivity analysis.</p> <p>Initial testing of methanol - air quality relationship.</p> <p>Explaining smog chamber results.</p>
Tier 2: Trajectory Modelling	<p>Relatively fast, computationally.</p> <p>Describes important atmospheric processes.</p> <p>Can test importance of emissions, deposition, meteorology and other physical phenomena.</p>	<p>Limitations in model formulation.</p> <p>Only provides information along a single trajectory.</p>	<p>Sensitivity testing of model inputs.</p> <p>Identifying particularly interesting cases for airshed modeling.</p> <p>Initial estimates of emissions - air quality relationships from converting to methanol.</p>
Tier 3: Airshed Modelling	<p>Complete description of atmospheric pollutant dynamics.</p> <p>Provided emissions - air quality relationships across entire basin.</p> <p>Minimal limitations in model formulation.</p>	<p>Computationally intensive.</p>	<p>Develop emissions - air quality relationship for the SoCAB.</p> <p>Primary source of determining expected impact from methanol use.</p>

Ozone is formed in the atmosphere by a complex series of reactions involving reactive organic gases (ROG) and nitrogen oxides (NO_x). A simplified scheme describing the roles of the different species is the three step sequence:



which shows how emissions of ROG and NO produce NO_2 , which then photolyzes ($h\nu$) in the presence of sunlight and oxygen (O_2) to form ozone (O_3). Reaction 1, the oxidation of the reactive organic by hydroxyl radical ($\text{OH}\cdot$), often controls the rate of ozone formation (i.e. it is the rate controlling reaction).

A simple measure of a source's ozone forming potential comes from multiplying the mass emissions of the individual organic exhaust species by that species' hydroxyl radical ($\text{OH}\cdot$) reaction rate constant to get a reactivity weighted emissions estimate. The principal organic exhaust component of methanol-fueled sources is unburned methanol, which is significantly less reactive than the mix of organics emitted from conventionally fueled sources (Alston, 1988; Snow et al. 1989). Therefore, less ozone is formed in a given amount of time. Figure 1.2 shows the mass emissions and reactivity weighted emissions of a conventionally fueled vehicle (CFV) and a comparable methanol fueled vehicle (MFV). Total mass emissions are equal, but the methanol emitted by the MFV is significantly less reactive. Unfortunately, this simple measure of the ozone formation potential does not take into account the other processes occurring in the atmosphere. Switching to methanol would alter the chemical production and cycling of other pollutants. Atmospheric transport and diffusion processes further affect the evolution and interactions of species' pollutants and precursors. The actual ozone formation process is a complex function which depends on the composition and levels of ROG and NO_x , and the prevailing meteorology. These complex interactions require a detailed analysis to accurately estimate the potential of methanol fuel usage to reduce ozone levels.

On-road motor vehicles contribute a significant share of ROG and NO_x emissions in urban areas, as shown in Figure 1.3. In the SoCAB, diesel fueled vehicles are forecasted to be responsible for 16% of the total NO_x in the year 2000 (Figure 1.3a). Methanol fueled diesel cycle vehicles emit about one half the NO_x as conventional diesels, so the possibility for a significant reduction in NO_x emissions exists. Combined with the lower organic reactivity, and hence slower oxidation of NO to NO_2 , lower ambient O_3 and NO_2 levels would be realized from conversion.

Sulfate and fine particulate matter (PM_{10}) levels could also be reduced by switching to methanol. Methanol contains little sulfur, so SO_x emissions from mobile and stationary sources would be greatly reduced. Aerosol nitrate would be decreased by lower NO_x emissions from diesel vehicles and stationary sources and from the lower reactivity of the organics. Conversion of diesel engines to methanol would remove emissions of primary organic and elemental carbon particulate matter, and the formation of secondary organic aerosol would also be reduced. Particulate matter, being composed of sulfate, nitrate, primary and secondary organics, and other compounds would decrease. As a result, visibility would improve.

KEY

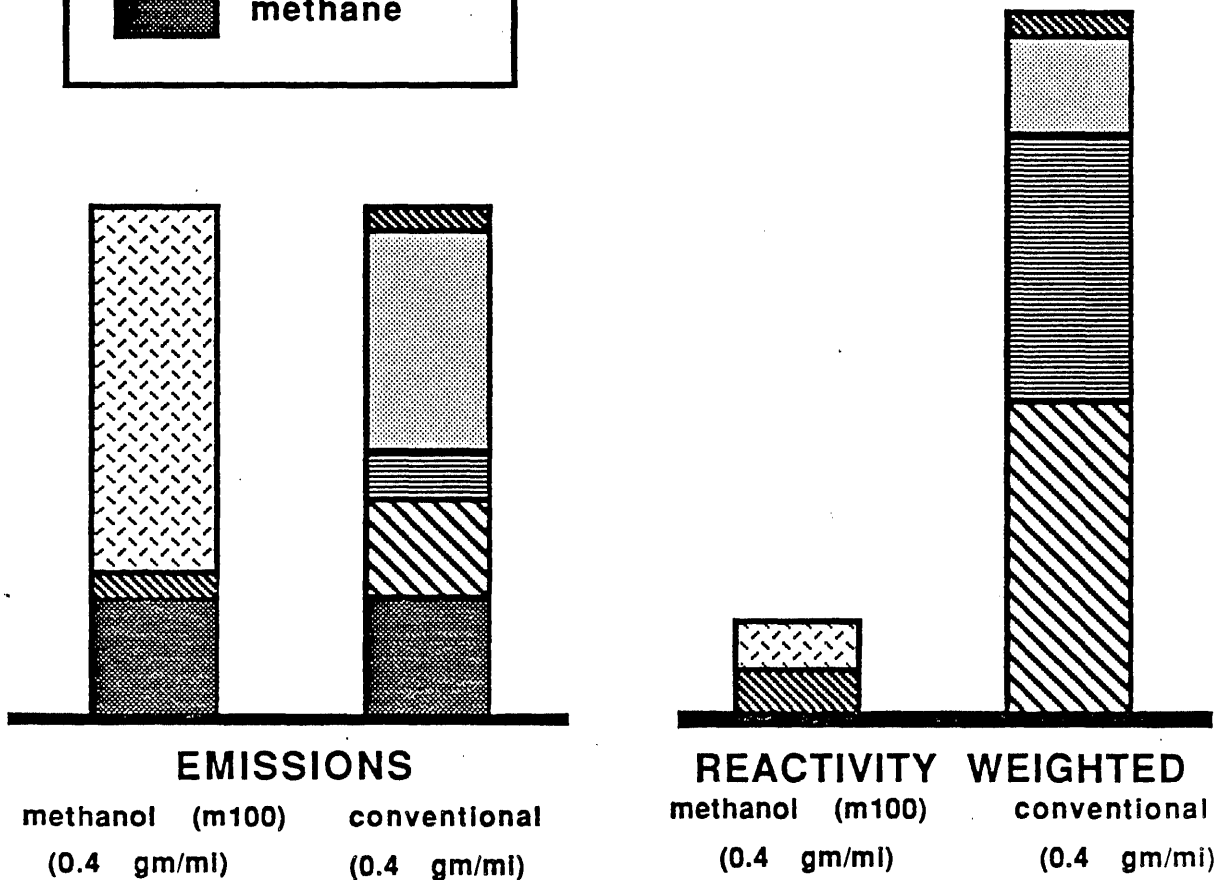
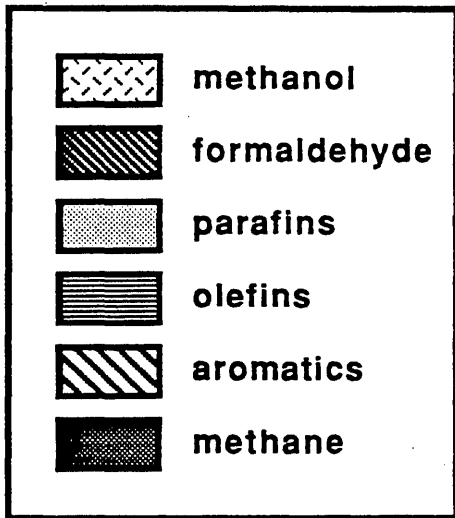


Figure 1.2 Comparison of the exhaust composition of an M100 MFV with corresponding emissions from CFVs. An estimate of the ozone forming potential can be obtained by multiplying the emission rate of individual components by their OH-reactivity. On this basis, MFV emissions are about 6-7 times less reactive than a comparable CFV. The resulting "Reactivity Weighted Emissions", however, does not include effects of other reaction paths or atmospheric dynamic variables. Thus, the need for a more detailed analysis.

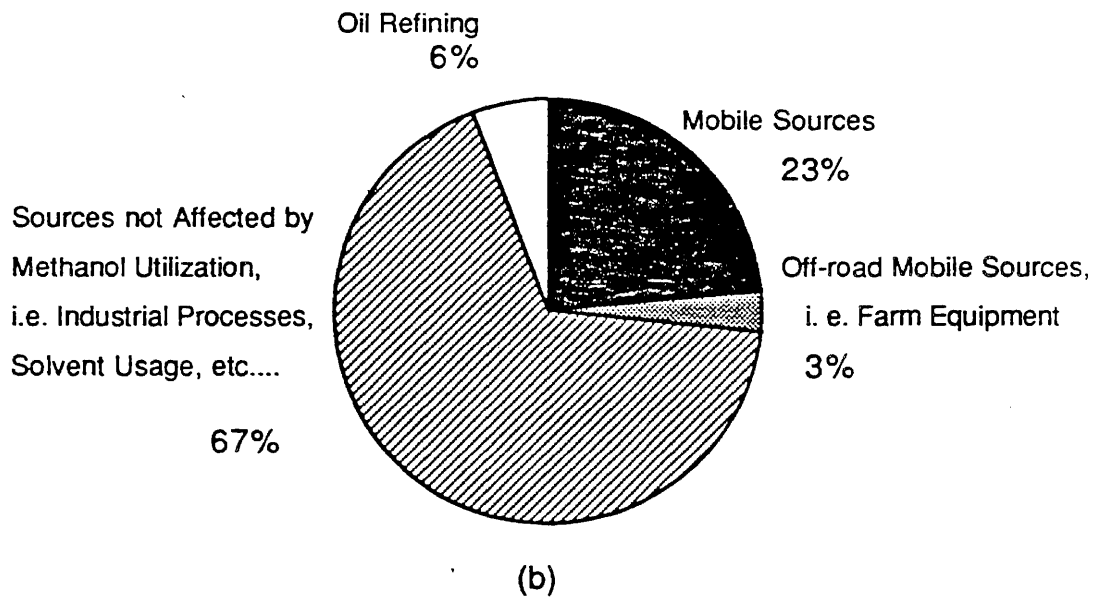
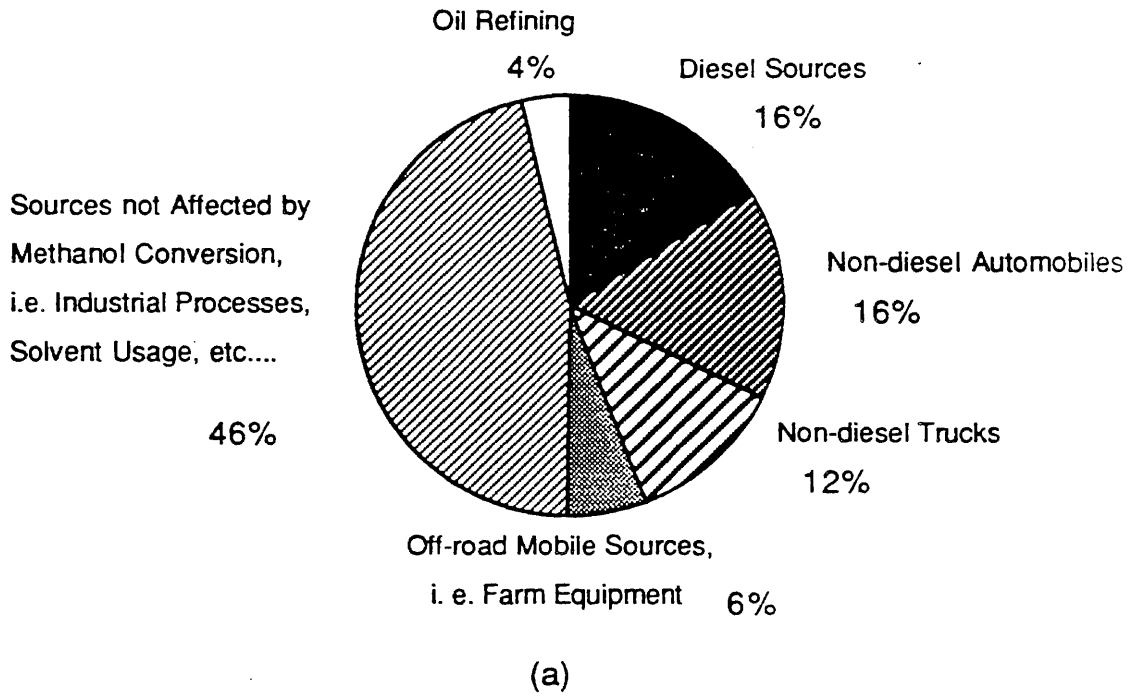


Figure 1.3 Emission Source Type Distribution in the Year 2000
(a) NO_x Emissions (b) ROG Emissions

Benzene, a carcinogen, is directly emitted by conventionally fueled vehicles. Ambient benzene levels have been measured up to 29 ppb (Grosjean and Fung, 1984). Motor vehicles are a primary source of benzene, which has led to concern about exposure during commuting. Control programs have been proposed to deal with this problem. Methanol fueled vehicles (MFVs) emit significantly less benzene, if any, so conversion would reduce ambient concentrations of this carcinogen.

In addition to reducing ozone concentrations and other compounds for which regulatory criteria have been set, methanol fuel use could potentially reduce acid deposition and levels of nitric acid, peroxyacetyl nitrate (PAN), suspected carcinogens such as polycyclic aromatic hydrocarbons (PAH), nitro-polycyclic aromatic hydrocarbons (NPAH), and benzene. Figure 1.3b portrays the percentage of ROG emissions that mobile sources are projected to contribute in the year 2000. Methanol fuel utilization would, however, increase ambient levels of methanol and its impact on ambient formaldehyde has been a subject of debate. Formaldehyde is an eye irritant and suspected human carcinogen. The potential for significant improvements and accompanying pitfalls mandate a detailed analysis of the quantitative effects of the air quality impact of methanol fuel usage.

1.4 Methodology of this Study

This study uses a three-tiered modeling approach to determine the atmospheric levels of photochemical pollutants such as ozone, formaldehyde, aerosol nitrate, peroxyacetyl nitrate (PAN), and nitric acid. The three tiers are developing and testing a chemical mechanism, performing a trajectory analysis of the basin, and conducting an airshed analysis of the basin. By separating the analysis into individual steps, each aspect can be investigated in greater detail, utilizing the strengths of each model type (Table 1.2). Adequately analyzing all the issues using a single model is prohibited by the high degree of non-linear interaction that would require excessive computational resources. The tiered modeling approach is a powerful and effective way to decompose the problem into a set of smaller problems, and thus evaluate the impact of various processes and uncertainties.

The first tier is the development and testing of a chemical mechanism. An accurate chemical mechanism is vital to a successful atmospheric modeling program. By focusing on the chemical processes only, possible bias from the meteorology and emissions can be removed from the analysis. This is a "zero dimensional analysis" of the problem, commonly called chemical kinetics modeling. It does not include any spatial change in pollutants. Formal sensitivity analysis is included in the evaluation to quantify the contribution of methanol and formaldehyde to ozone formation. This allows for more detailed comparison to other mechanisms.

After a suitable mechanism has been obtained and tested, it is incorporated into a trajectory formulation of the atmospheric model. This is the second tier of the approach. The trajectory model uses a control mass, or Lagrangian, formulation of the reaction-diffusion-advection equation, where a single air parcel is tracked as it moves through the basin. The model includes the effects of meteorology, vertical diffusion, chemistry, and emissions, but neglects wind shear and horizontal diffusion from adjacent air parcels. It is a two dimensional analysis of the problem (horizontal and vertical pollutant transport). Because it considers only one air parcel in the entire basin, it is computationally around 200 times faster than an analysis of the entire basin using the Eulerian, grid-based airshed model. Though many more simulations can be run with the trajectory model it does not provide information across the entire the basin. It computes pollutant concentrations at one location in time and space along an air parcel path.

A large number of possible emissions scenarios are analyzed with the trajectory model. These scenarios have been used to develop a preliminary estimate of air quality impacts, calculation of secondary organic aerosol formation, sensitivity analysis, and, particularly, to suggest which conditions should be investigated in greater detail using the grid-based airshed model. The airshed model is a control volume, or Eulerian, formulation of the reaction-diffusion-advection equation, and is the most complete description of the processes affecting the evolution of pollutants in the atmosphere. In this study, the modeling region covers the entire basin and is a fully three-dimensional analysis of the problem. The airshed model is computationally intensive, but it provides for a very complete analysis and has minimal restrictions in model formulation. Evaluating a large number of scenarios with the trajectory model and testing only specific ones with the airshed model is more efficient than using either model alone. Obtaining information as efficiently and thoroughly as possible is the purpose of the three-tiered approach to this problem.

Not all pollutants affected by methanol use are effectively treated by the three-tiered photochemical modeling structure just described. Primary organic and elemental carbon particulate are best studied using non-reactive models. Wintertime build-up of methanol and formaldehyde, and the decrease in ambient benzene, is treated using historical CO concentrations and emissions rates and assuming linear relationship. Future sulfate concentrations are estimated using results from the recent Air Quality Management Plan (AQMP) (SCAQMD and SCAG; 1988). The impact on PM₁₀ is found by integrating the results on how methanol will affect individual particulate species.

1.5 Outside Project Participation

A notable aspect of how this project was conducted was the in-progress meetings held jointly by CARB and CMU. These meetings were open to outside participation and attended by representatives of interested parties, such as gas and oil companies, motor vehicle manufacturers, electric utilities, regulatory agencies, academia, and consulting firms. Attendees were asked to openly discuss and criticize, both positively and negatively, aspects of the study and to suggest future direction. The stipulation of the meeting was that interim results were not to be disseminated before publication by CMU or CARB. The intent was to provide as much feedback as possible between CARB, CMU, and those who would be affected by regulatory reaction to the project results. The study has benefitted from those meetings, and suggestions have been incorporated when possible.

Many of the calculations performed are the results of these meetings and decisions of the Clean Fuels Working Group (CFWG, formerly the Methanol Task Force, comprised of representatives of the California Energy Commission, SCAQMD and CARB). Specific future scenarios were specified by members of CARB and the CFWG after reviewing input from the CMU team and the meetings. The Mobile Source Division staff of CARB provided detailed emission factors for future automobiles and trucks, accounting for their knowledge of expected future regulations and technologies. After specification of the emission factors and scenarios and open discussion during the in-progress meetings, CMU executed the analysis.

1.6 Previous Studies: Results and Limitations

Interest in utilizing methanol in mobile and stationary sources was generated in the late 1970's and early 1980's in response to the fuel crisis. Methanol was in consideration as a primary fuel or as an additive to gasoline. Since that time, a variety of studies have addressed the question of its environmental impact (e. g. Pefley et al., 1984; O'Toole et

al., 1983; Bechtold and Pullman, 1980; Balentine et al., 1985; Carter et al., 1986a; Whitten and Hogo, 1983; Whitten et al., 1986; Norbeck and Nichols, 1986). These studies used chemical kinetic models, air quality models, environmental smog chambers, and smog chamber simulations. These studies concentrated primarily on ozone formation. Interpretations of the results of these studies have been conflicting, and the technology and assumptions involved have been criticized for having significant limitations.

1.6.1 Mathematical Modeling Studies

Photochemical smog formation results from a complex system of competing, non-linear processes which occur simultaneously in the atmosphere. It is impossible to analytically determine air quality impacts, therefore, numerical modeling analysis, i. e. photochemical air quality modeling, is commonly used. Various types of models have been used in previous studies. Balentine et al. (1985) used a zero dimensional, chemical kinetics modeling approach, while O'Toole et al. (the JPL study; 1983), Norbeck and Nichols (Ford Twenty Cities Study; 1987), and Whitten and Hogo (SAI 1; 1983) and Whitten et al. (SAI 2; 1986) used box, trajectory, and/or grid-based, Eulerian models.

The first modeling study by Systems Application Incorporated (SAI 1), (Whitten and Hogo, 1983) investigated the potential air quality benefits of methanol in the Los Angeles region. An EKMA (level II) one day trajectory model was used to address the impact on ozone in the SoCAB. Various levels of formaldehyde in the exhaust of methanol fueled sources were considered, however, changes in emissions inputs into the model were not treated in detail. They also directly tested the sensitivity to initial conditions, MFV exhaust formaldehyde content, and methyl nitrite emissions. Ozone was reduced up to 31% from 0.273 ppm to 0.188 ppm, using the forecast 1987 inventory as a base case. They found a strong sensitivity to exhaust formaldehyde content. Predicted peak O₃ was 0.188 ppm for no HCHO (formaldehyde) in the exhaust, 0.213 ppm for 10% HCHO in the exhaust, and 0.237 for 20% HCHO in the exhaust. However, tests showed a strong sensitivity to initial and boundary conditions (both of which will change given a large scale conversion to MFVs). When initial and upper level organic gas concentrations were halved, ozone was reduced to 0.181 ppm.

The JPL study modeled a one day trajectory traversing the SoCAB. The study looked at the impact of methanol fuel utilization on air quality in the year 2000. A 1974 inventory for the SoCAB was scaled forward, accounting for expected automotive emission controls and economic growth. However, stationary source emissions were not changed, nor was the spatial distribution of emissions. They did account for changes in fuel vapor pressure and composition of evaporative emissions. The model employed was the CIT (Carnegie Institute of Technology/California Institute of Technology) trajectory model, a predecessor of the one used in the present study. A single air parcel trajectory, less than twenty-four hours in extent, was used for their study.

A number of cases were evaluated as part of the JPL study, including complete substitution of methanol vehicles for gasoline (not diesel) fueled vehicles in the year 2000 assuming: 1) same ROG and NO_x emissions rates as of gasoline, 2) same ROG emissions rates, NO_x emissions rates at 50% that of gasoline 3) 50% reduction of both ROG and NO_x. The composition of the MFV exhaust was 72.7% methanol, 21.2% formaldehyde, and 6.1% alkane by mass. They found that with complete substitution with MFVs emitting at the same rate as CFVs (case 1), ozone was reduced from 0.333 ppm to 0.285 ppm (14.4%). Greater reductions were found for cases 2 and 3, with 17.4% and 19.8% reductions, respectively. If no automotive emissions were used, the reduction was 25%. Thus, even with the rather large fraction of formaldehyde in the exhaust (21% vs. ≈

1-10%, as used here), methanol was found to be effective at reducing O₃, lowering the predicted O₃ by about 60% of the amount calculated if all gasoline fueled vehicle emissions are removed.

Though the JPL study was very detailed in its treatment of emission inputs, it has been criticized. First, the air parcel studied was tracked for less than twenty-four hours, and thus the results were very sensitive to initial conditions. As listed in Table 1.2 and discussed later, trajectory models themselves also have limitations in their formulation. The formaldehyde fraction of the exhaust is higher than current data would suggest, and much higher than the possible regulatory levels. On a reactivity basis, the formaldehyde fraction of their MFV exhaust overwhelms the methanol fraction. Finally, more recent and detailed data is now available for future emissions from mobile and stationary sources.

Other modeling studies have concentrated on the effects of methanol fuel substitution outside of the SoCAB region. The chemical kinetic modeling by Balentine et al. (1985) was conducted to test the applicability of various mechanisms for inclusion in models. The results showed decreases in ozone resulting from methanol use. Ford Motor Company modeled 20 cities with an EKMA type trajectory model. This study assumed immediate penetration of MFVs into the fleet. They found that ozone was reduced by 1 to 36% in cases where the MFV exhaust was 0% formaldehyde, and by 0 to 13% in cases where the exhaust was 10% formaldehyde. SAI 2, (Whitten et al., 1986) used three different models to study the impact in Philadelphia, but in each case, results were sensitive to the initial and or boundary conditions. That study indicated little or no benefit from MFV substitution.

The results from all of the above studies highlight a number of important points. Methanol utilization appears to be effective at reducing ozone under certain circumstances. Secondly, the exhaust formaldehyde fraction is the dominant contribution to O₃ formation. Finally, modeling as done in the JPL and SAI studies can be very sensitive to initial conditions, and care must be taken in specifying trajectory paths and modeling regions.

1.6.2 Experimental Studies

The University of California, Riverside Statewide Air Pollution Research Center (SAPRC), performed a series of well documented, methanol-related smog chamber experiments in a 6,400 liter indoor Teflon chamber (ITC) and a 50,000 liter outdoor Teflon chamber (OTC), (Carter et al., 1986a). Pollutants similar to that in a very dirty urban atmosphere were introduced into a chamber and the pollutant concentrations were followed over time periods of up to three days. This was done for pollutant mixes corresponding to current emissions and also for mixes corresponding to methanol fueled engine emissions replacing one third of the base mixture. On the first day, peak ozone levels were significantly lower for the methanol emissions mix than for the conventional emissions mix. However, this difference decreased over time, and ozone levels were similar by the third day. This result raised the question about methanol impacts during multiday smog episodes. It was thought that methanol could build up, negating any benefits, and that a large fraction would react within three days.

In a previous study, the University of North Carolina (Jeffries et al., 1985) conducted 29 smog chamber experiments involving methanol with varying levels of formaldehyde. One third of the "base" organic mixture was replaced with a methanol or a methanol-formaldehyde mixture, either a 90:10 CH₄O:HCHO ratio or a 80:20 CH₄O:HCHO ratio. Ozone reductions varied widely, from 0-80% depending on the HCHO content and organic loading.

An earlier smog chamber experiment (Pefley et al., 1983) also looked at methanol substitution. However, the conditions were atypical of urban conditions and used isobutene, not formaldehyde, as part of the MFV exhaust composite. Again, the one day experiments suggested ozone would be reduced from methanol substitution.

Differences between smog chambers and the atmosphere make it difficult to use smog chamber results for predicting basin wide air quality changes. One difference is that a smog chamber does not replicate atmospheric diffusion and transport of chemical species. A second difference is that for the experiments conducted all pollutants were present at the beginning of the smog chamber experiments. Conversely, fresh pollutants are being emitted throughout the day into the atmosphere. Consequently, the smog chambers had very low NO_x concentrations on days two and three of the simulations making ozone levels relatively insensitive to changes in ROG. A third difference is that even a very large smog chamber has a surface area to volume ratio many orders of magnitude greater than the atmosphere, and surface reactions have a much larger effect on pollution formation in the smog chamber than they do in the atmosphere. While these tests are extremely valuable for investigating certain aspects of atmospheric chemistry, they cannot be used to directly predict the effects of various emissions control strategies, especially for multiday episodes. Due to the limitations of these and other previous studies, a more rigorous approach, as present in the three-tiered modeling study developed for this study, is necessary.

1.7 Organization of this Report

Development and implementation of the three-tiered photochemical modeling approach is covered in the next five chapters of this report. The next two chapters investigate two special issues, aerosol formation and wintertime pollutant build-up, in further detail. The final two chapters present recommendations for future studies and a summary and conclusions. A brief description of the topics covered in the report chapters follows.

Chapter 2 introduces the chemical mechanism for modeling urban atmospheres affected by emissions of both conventionally and methanol fueled sources. Evaluation of the mechanism against a suitable set of environmental chamber experiments is reviewed to determine the performance and its suitability for inclusion in air quality models.

After the mechanism is tested against experimental data, the sensitivity of the mechanism to various parameters is analyzed. This is described in Chapter 3. The sensitivities of this mechanism are also compared to the sensitivities of a second, recently developed, mechanism. Atmospheric reactions involved in ozone formation are highly nonlinear and dependent on local conditions. Sensitivity analysis is powerful for comparing the effects of various compounds on atmospheric pollutant concentrations.

Air quality models require information on emissions and meteorology. The treatment of emissions for the base case calculations and for scenarios involving utilization of methanol is covered in Chapter 4. Also, the three day episode that serves as the modeling period is described. Other inputs required by the air quality models are also covered.

In Chapter 5 the photochemical trajectory model is used to determine preliminary estimates of the air quality implications of extensive methanol utilization. Scenarios simulating a variety of possible emissions levels from MFVs and CFVs are investigated using three different air parcel trajectories. Each trajectory is affected by different source

types and emission rates, with the result that the same scenario in the different trajectories will produce different responses. The trajectory model is used to determine the effects that changes in emissions, ground level deposition rate, traffic timing, and initial conditions have on atmospheric concentrations of ozone, formaldehyde and PAN. In essence, this extends the sensitivity analysis started in Chapter 3. These calculations are used to provide a preliminary view of how methanol based strategies will affect air quality in the basin. Information derived from this section was used to suggest particular calculations for further analysis using the airshed model.

In Chapter 6, the grid-based airshed model is used to develop the basin wide response to utilizing methanol in mobile and stationary sources. In particular, quantitative estimates are provided for how ozone, PAN, NO₂ and formaldehyde formation will be affected by various levels of emissions from conventional and methanol fueling of motor vehicles and stationary sources. These calculations are performed for emission estimates corresponding to the years 2000 and 2010. These years were chosen as being the earliest dates at which methanol fueled vehicles could replace a significant fraction of the motor vehicle fleet.

Chapter 7 considers the effects of the emissions scenarios on aerosol levels in the basin. First, changes in primary fine total carbon and fine elemental carbon levels are analyzed. The 24-hr averaged concentrations of these compounds are from direct emissions, so a source-receptor analysis is used to determine levels as a function of emissions. Fine elemental carbon comes largely from diesel engine emissions, so converting these vehicles to methanol fuel can drastically change ambient levels. Next, levels of aerosol nitrate are determined for various methanol penetration scenarios. These calculations are done with the airshed model. Secondary organic aerosol levels in the basin are calculated as a function of emissions using a modified version of the photochemical trajectory model used in Chapter 5. Finally, changes in aerosol sulfate levels are estimated.

Chapter 8 analyzes wintertime levels of methanol and formaldehyde. In the winter, emissions react more slowly and mixing and dilution are reduced. A buildup of primary emissions beyond that which occurs in the summer becomes possible. It is necessary to determine if these species would be present in levels that could cause a potential health hazard.

The results of Chapters 5 through 8 are combined to form conclusions as to the potential benefits of methanol fuel conversion and to identify areas of uncertainty. Chapter 9 presents recommendations for future studies to address uncertainties identified in this study. Chapter 10 presents a summary and conclusion to this study.

2.0 Chemical Mechanism Evaluation

2.1 Introduction

A description of atmospheric chemistry, as shown in Figure 1.1, is an integral part of the three-tiered approach for estimating the response of air quality in the SoCAB to displacing conventional fuels with methanol. This chapter presents the chemical mechanism used in this study to represent atmospheric chemistry. A description of the procedures by which the mechanism was tested for its ability to simulate atmospheric chemistry, especially when high concentrations of methanol are present, follows. As part of the analysis, the mechanism is compared against a second chemical mechanism released since the beginning of this study. The final section of this chapter contains conclusions as to the suitability of the mechanism based on these test results. Further testing of the mechanism, using sensitivity is presented in Chapter 3.

The chemical mechanism describes the interactions between compounds in the atmosphere, and is at the heart of the ability of any model to accurately duplicate atmospheric processes. Therefore, the mechanism must include all significant atmospheric chemical reactions. In order to demonstrate its accuracy, the chemical mechanism used in this study was tested separately before being incorporated into the photochemical air quality models. By testing the chemical mechanism independently, the effects of other atmospheric processes are removed, and it is possible to analyze the strengths and weaknesses more effectively. In this case, the model predictions are evaluated against a series of experiments performed at the University of California, Riverside, Statewide Air Pollution Research Center. The design of these experiments allows for testing chemical mechanisms' performance in the presence of large amounts of methanol. Also, its sensitivity to experimental conditions is compared to another chemical mechanism. This extends the analysis of the chemical mechanism, and is the first part of the tiered approach used in this study where components of the model are tested at various levels independently before incorporating them into higher level models.

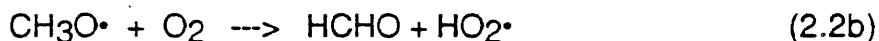
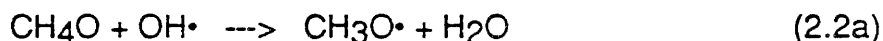
2.2 Chemical Mechanism

The chemical mechanism used in this study is a modified version of the Caltech mechanism (Falls and Seinfeld, 1978; Falls et al., 1979). The Caltech mechanism was selected because it was the mechanism used in a multi-day modeling study of an ozone episode that occurred in the SoCAB in 1982 (e.g. Russell et al., 1988). In that study and previous studies (McRae, 1983; Russell and Cass, 1983, 1987), models using the Caltech mechanism were able to predict the diurnal and spatial evolution of pollutants as a function of meteorology and emissions input. Further testing has shown that its predictions compare favorably with laboratory experiments and other mechanisms (Milford et al., 1988; Leone and Seinfeld, 1985). The Caltech mechanism has been extended to include methanol chemistry, an updated understanding of nighttime chemistry, and reaction rates and products have been updated to reflect recent findings including new photolytic rates. Also, it now includes modifications suggested by Leone and Seinfeld (1985). The new mechanism (called the Extended Caltech mechanism) uses a lumped species technique to obtain a balance of completeness and speed of solution.

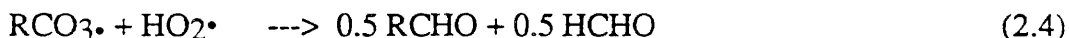
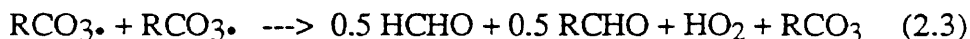
The Extended Caltech mechanism, as used in smog chamber modeling, is a series of 75 reactions involving 34 compounds, including lumped organic molecules and counter species. Methanol chemistry has been added, and is treated explicitly with the reaction:



which is a condensation of two reactions:



where the dot (\cdot) denotes a radical. Equation 2.2a is the rate controlling reaction of the pair. The reaction rate and activation energy used for this reaction is taken from Carter et al. (1986a). Preliminary mechanism testing against the smog chamber experiments indicated that the peroxy radical reactions with themselves are important for multiday simulations because the system becomes NO_x limited, with very little NO present at night. Following the work of Carter et al. (1986b), two reactions were added to account for acylperoxy radical loss at night under low NO conditions:



Reaction rates suggested by Carter et al. (1986b) were used. The primary effect of adding these reactions was to decrease PAN concentrations at night.

The 75 reactions and the rate constants used are given in Table 2.1. Ten of the reactions are photolytic, and are noted. The rate constants for photolytic reactions were taken from Carter et al. (1986a,b), and depend on experimental conditions. Six additional reactions, also noted, model radical reactions with the smog chamber walls. They are included in the mechanism when modeling smog chamber experiments, but are deleted when modeling the atmosphere. Two reactions involving isobutene were included for smog chamber modeling because of the addition of isobutene as a surrogate for formaldehyde in the base organic mixture. Likewise, these reactions are not included in the atmospheric models. The reaction rates for the wall radicals come from Carter et al. and are different for the indoor teflon chamber (ITC) and the outdoor teflon chamber (OTC). Also, a constant dilution rate, specified in Carter et al. (1986b) was included in the ITC modeling runs because the ITC appeared to have a small leak. Many of these rate constants have been updated since the CIT mechanism was originally released, with the new values coming primarily from Carter et al. (1986b), Atkinson and Lloyd (1984) and Baulch et al. (1982).

2.3 Mechanism Evaluation

Once a mechanism has been created, it must be tested to determine if it is an accurate representation of the chemical processes. This validation can be done in two different ways. It can be tested by modeling chamber experiments and then comparing the model's predicted results against the actual results. Also, it can be tested mathematically, by testing its sensitivity to changes in system parameters, and comparing these results to explicit, well evaluated mechanisms. Both of these are done here. The experimental study selected for testing is presented in the next section, followed by the results of the comparison.

Table 2.1 Chemical Mechanism

Reactants		Products	Reaction Rate	Activ. Energy	Notes
NO2	→	NO + O3P	0.326	0	P
O3P + O2	→	O3 +	0.000021	-510	
O3 + NO	→	NO2 + O2	24.5	1450	
NO2 + O3P	→	NO + O2	13300	0	
NO + O3P	→	NO2	3900	-584	
NO2 + O3P	→	NO3	2940	0	
O3 + NO2	→	NO3 + O2	0.0491	2450	
NO3 + NO	→	2 NO2 +	29400	0	
NO + OH	→	HONO + LX1	16900	0	
HONO	→	OH + NO + SX1	0.106	0	P
HO2 + NO2	→	HONO + O2	0.165	-1006	
HONO + OH	→	NO2 + H2O + LX2	9690	0	
NO2 + HO2	→	HNO4	1650	-1006	
HNO4	→	HO2 + NO2	7.23	9950	
HO2 + NO	→	NO2 + OH + SX2	11900	0	
RO2 + NO	→	2 NO2 + RCHO + 2 HCHO	6000	0	
RCO3 + NO	→	NO2 + RO2 + CO2	3760	0	
NO2 + OH	→	HNO3 + LX3	15400	0	
CO + OH	→	HO2 + CO2 + LX4	436	0	
O3	→	O3P + O2	0.00167	0	P
HCHO	→	2 HO2 + CO	0.00076	0	P
HCHO	→	H2 + CO	0.00241	0	P
HCHO + OH	→	HO2 + LX5 + CO	13900	0	P
RCHO	→	RO2 + HO2	0.00007	0	P
RCHO + OH	→	RCO3 + H2O + LX6	17000	0	
C2H4 + OH	→	RO2 + LX7	11700	0	
C2H4 + O3P	→	RO2 + HO2	1220	0	
OLE + OH	→	RO2 + LX8	37200	0	
OLE + O3P	→	RO2 + RCO3	0.591	0	
OLE + O3	→	RCHO + HCHO + 1.64 HO2	0.0083	0	
ALK + OH	→	RO2 + LX9	4500	0	
ALK + O3P	→	RO2 + OH + SX3	0	0	
ARO + OH	→	RO2 + RCHO + LX10	36200	0	
RO	→	HO2 + 0.5 HCHO + 0.5 RCHO	200000	0	
RONO	→	NO + RO	0.0652	0	
RO + NO	→	RONO	14600	0	
RO + NO2	→	RNO3	7300	0	
RO + NO2	→	RCHO + HONO	0	0	
NO2 + RO2	→	RNO4	5460	0	
NO2 + RO2	→	RCHO + HNO3	0	0	
RNO4	→	NO2 + RO2	7.23	9950	
RCO3 + NO2	→	PAN	2060	0	
PAN	→	RCO3 + NO2	0.0371	12516	
NO2 + NO3	→	N2O5	2490	0	
N2O5	→	NO2 + NO3	3.79	0	
H2O + N2O5	→	2 HNO3	1.89E-06	11080	
O3 + OH	→	HO2 + O2 + LX11	78.8	0	
O3 + HO2	→	OH + 2 O2 + SX4	2.34	1000	
HO2 + HO2	→	H2O2 + O2	7110	580	
H2O2	→	2 OH + SX5	0.00029	0	P
RO2 + RO2	→	1 RCHO + HO2 + 0.7 HCHO	73.9	0	
NO3 + HCHO	→	HNO3 + HO2 + CO	0.86	0	
NO3 + RCHO	→	HNO3 + RCO3	3.6	0	
NO3	→	NO2 + O	0.0117	0	P
NO3 + OLE	→	HNO3 + RCO3	10.1	0	
NO2 + NO3	→	NO2 + NO	0.583	0	
CH4O + OH	→	HCHO + HO2	1380	0	
OLE + O3	→	2 RO2 + 0.8 OH + 0.7 CO	0.0083	0	
A	→	A + OH	0.000065	0	P,W
NO2	→	1 NO + 0.5 LX12	0	0	
NO2	→	NO + LX12	0	0	

Table 2.1 Chemical Mechanism, cont...

Reactants		Products	Reaction Rate	Activ. Energy	Notes
O3	→		0.00013	0	W
A	→	A + NO2	0.000033	0	P,W
RO2 + NO	→	2 HO2 + LX13	6000	0	
RO2 + HO2	→	ROOH + LX14	4400	0	
NO2	→	HONO + B	0.00014	0	W
NO2 + B	→	HNO3	100000	0	
LX14	→	LX14 + LX15	10	0	
ROOH	→	HO2 + OH	0.000295	0	
N2O5 + H2O	→	LX12	5E-08	0	W
N2O5	→	LX12	0.0025	0	W
ISOB + OH	→	ISOR + HCHO + RCHO	76000	0	
ISOR + NO	→	NO2 + OH + HO2	10000	0	
RCO3 + HO2	→	1 HCHO + 0.5 RCHO	4434	0	
RCO3 + RCO3	→	1 HCHO + 0.5 RCHO + HO2	3670	0	

NOTES

P Photolytic reaction, or reaction rate dependent on photolytic flux. Values shown are for ITC simulations. Values for OTC experiments vary diurnally, and are taken from Carter et al. (), and experimental logs.

W Wall dependent reaction. Value shown is for ITC simulations.

2.3.1 SAPRC Smog Chamber Experiments

The University of California, Riverside Statewide Air Pollution Research Center (SAPRC) performed a series of well documented smog chamber experiments to investigate the effects of methanol fueled source emissions on atmospheric air quality (Carter et al., 1986a). The SAPRC study ran both indoor and outdoor experiments in teflon chambers. Indoor teflon chamber (ITC) experiments have the advantage of being more controllable and having greater repeatability. Outdoor teflon chamber (OTC) experiments have conditions that much more closely resemble the atmosphere, but day to day meteorological variations make duplication impossible.

For the ITC runs, a sample of polluted 'air' is put in a 6,400 liter teflon chamber. The chamber has rows of ultraviolet lights on two sides and a fan in the chamber to circulate the mixture. During the experiments, the lights are turned on for 12 hours each day. Before each experiment, the bag is flushed out several times with pure dry air. At the beginning of the experiment various pollutants and pollution causing compounds are injected into the chamber. The concentrations of the species of interest are measured throughout the experiment. Chamber design and testing techniques were done in an attempt to minimize any reaction of chamber contents with anything except other contents. However, it is not possible to remove everything from the chamber walls and reactions between the experimental mixture, the wall, and contaminants on the wall do occur. The SAPRC experimenters quantified these reactions and other chamber dependent parameters by running chamber characterization tests. A more detailed description of the ITC test equipment and test techniques can be found in section III A of Carter et al. (1986a).

The primary piece of equipment used in the OTC experiments was a 50,000 liter teflon chamber. The chamber was divided in half by pinching it between metal rods. Side A of the divided chamber was on the eastern half and side B was on the western half. To keep sunlight from reaching the bag when it was not wanted, the two halves were covered by tarpaulins stretched over a supporting framework. The bag was usually only uncovered between 9 AM and 3 PM (PST) to prevent preferential radiation of the eastern half over the western half and vice versa. The bag was raised off the ground to let air circulate beneath. When the experimenters wanted to mix the contents of the bag, they would agitate the sides of the bag manually. Solar radiation intensity and k_1 measurements were taken only for the whole system, not both sides independently. As with the ITC runs, the design of the equipment and the experimental techniques were done in order to minimize the contamination of the test mixture. The OTC was sampled less frequently than the ITC to prevent excessive depletion of the bag's contents. A more detailed description of the OTC setup and experimental procedures is given in section III B of Carter et al. (1986a).

In addition to running the ITC and OTC experiments, the SAPRC experimenters also developed and ran a computer model of their test cases. The SAPRC model is an explicit mechanism, i.e. it keeps all molecules distinct (or nearly so) instead of lumping, and as a result it has approximately 300 reactions for a relatively simple test mixture. Thus, the Extended Caltech mechanism can be compared to experimental data and the more inclusive, newer model. This is useful when the experimental results differ from the model predictions obtained with both the Extended Caltech mechanism and the SAPRC explicit mechanism. If this is the case, the source of disagreement is considered to be an incomplete understanding of the chamber conditions, as opposed to a weakness in one mechanism as compared to the other.

Smog chamber results are dependent on a variety of poorly understood processes. In particular, wall related reactions can be a major source of radicals. The source rate of the

radicals and their impact is parameterized from analysis of a number of tests, though the fundamental process is not well understood. Other uncertainties also contribute to modeling error. For example, there was a suspected leak in one of the chambers. In another instance, OTC run 240, k_1 values were inconsistent with other test data and the experimenters noted their doubts about the data in the test logs. In this run the k_1 values were scaled to the uv radiation data and the results showed reasonable (although below average) agreement with the test data. It is also difficult to measure formaldehyde at low concentrations. Smog chamber measurements of HCHO show considerable scatter, though the predictions agree reasonably well, both in magnitude and timing, with the HCHO observations.

2.3.2 Test Results

2.3.2.1 ITC Test Results

Fourteen ITC runs were analyzed. Table 2.2 shows the ROG/NO_x ratios of these runs and the makeup of the ROG. Four types of ROG mixtures were used in the SAPRC study. The base case used a surrogate organic species mix to represent that found in polluted urban atmospheres. The methanol plus formaldehyde substitution case replaced, nominally, one third of the base case mix with a mixture of 90% methanol and 10% formaldehyde. Next, the methanol only case replaced one third of the base case mix with methanol. Finally, the blank substitution case reduced the amount of the base case mix by one third.

Predicted and observed peak ozone concentrations are shown in Table 2.3.a and 2.3.b for days 1 and 2, respectively. Except for runs 868 and 871, the Extended Caltech mechanism predicted the SAPRC measured peak ozone closely. For the first day, runs with ROG/NO_x ratios greater than 3.0 show agreement within 20% on all but two runs. On the runs with ROG/NO_x ratios equal to 3.0, the measured and predicted ozone concentrations are both low. On the second day, all runs with ROG/NO_x ratios greater than three agree within 20%. The model and SAPRC peak ozone concentrations are plotted against each other in Figures 2.1.a and 2.1.b. Figure 2.2 plots the model and SAPRC peak ozone concentrations versus ROG/NO_x ratios. This indicates that there is a very strong correlation between ROG/NO_x ratio and peak ozone magnitude. A review of SAPRC test logs for ITC runs 868 and 871, the two with the worst agreement between the model and SAPRC data, indicate that the initial formaldehyde concentration may not have been 0 ppm, as it was supposed to be. If initial conditions corresponding to the measured values are used, the model predicts higher ozone concentrations and brings the two into closer agreement. However, in their report, Carter et al. (1986a) using the SAPRC explicit mechanism, used 0 ppm initial formaldehyde concentrations on these two runs. This path was then adopted here. In run 871 the explicit model also underpredicted the peak ozone concentration.

Levels of ozone, PAN and HCHO versus time were plotted for run ITC 872. These are shown in Table 2.4 and in Figure 2.3. The Extended Caltech mechanism predicted PAN concentrations higher than the SAPRC measured levels. This is consistent with the inclusion of PAN analogues in the mechanism lumped species PAN. The predictions obtained with the Extended Caltech mechanism show good agreement with the SAPRC experimental data for ozone and formaldehyde in both magnitude and timing.

Table 2.2 NO_x/ROG Ratios of ITC Runs

ITC Run No.	ROG/NO _x Ratio		ROG Mixture
	Nominal	Actual	
865	15.0	16.7	baseline
891	15.0	14.5	baseline
867	15.0	14.8	MeOH+HCHO
888	15.0	14.4	MeOH
868	15.0	8.2*	Reduced Base
871	6.0	5.1	Baseline
872	6.0	6.0	MeOH+HCHO
877	6.0	5.6	MeOH+HCHO
874	6.0	6.0	MeOH
873	6.0	3.8*	Reduced Base
880	3.0	3.1	Baseline
881	3.0	3.1	MeOH+HCHO
886	3.0	3.1	MeOH
885	3.0	2.3*	Reduced Base

* ROG/NO_x Ratio reduced because about one third the organic is removed in the reduced base case simulations.

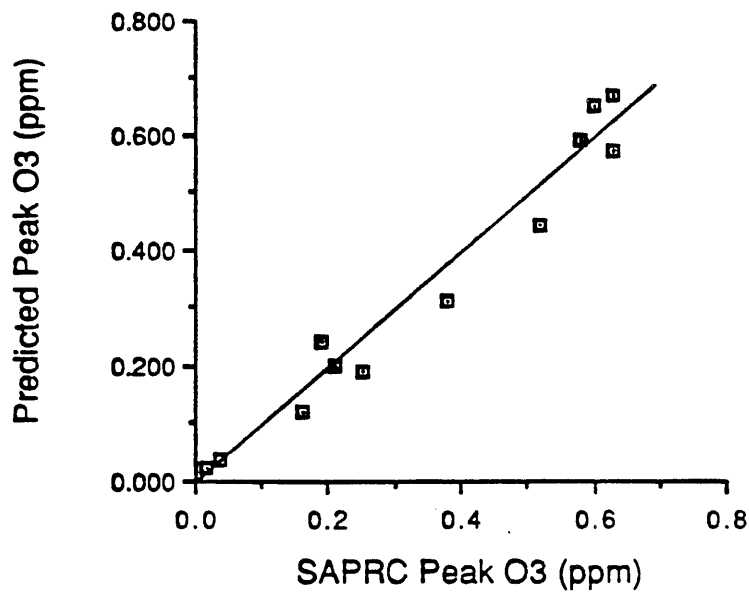
ITC Run Number	SAPRC Experimental Peak Ozone Conc.		Calculated Peak Ozone Conc.	
	(ppm)	time (hrs)	(ppm)	time(hrs)
865	.63	8	.67	8
867	.63	12	.57	12
868	.52	12	.44	12
871	.38	12	.31	12
872	.21	12	.20	12
873	.16	12	.12	12
874	.19	12	.24	12
877	.25	12	.19	12
880	.03	12	.03	12
881	.01	12	.02	12
885	.01	12	.02	12
886	.01	12	.02	12
888	.58	12	.59	12
891	.60	12	.65	9

(a)

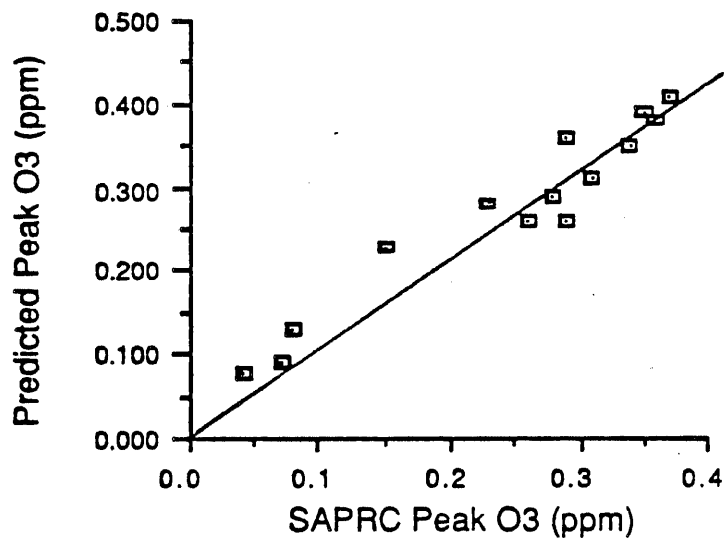
ITC Run Number	SAPRC Experimental Peak Ozone Conc.		Calculated Peak Ozone Conc.	
	(ppm)	time (hrs)	(ppm)	time (hrs)
865	.37	24	.41	36
867	.36	36	.38	36
868	.29	36	.36	36
871	.31	36	.31	36
872	.23	36	.28	36
873	.26	36	.26	36
874	.28	35	.29	36
877	.29	36	.26	36
880	.15	36	.23	36
881	.08	36	.13	36
885	.04	36	.08	36
886	.07	36	.09	36
888	.35	36	.39	36
891	.34	36	.35	36

(b)

Table 2.3 Predicted and Observed Ozone Concentrations
(a) Day 1 (b) Day 2

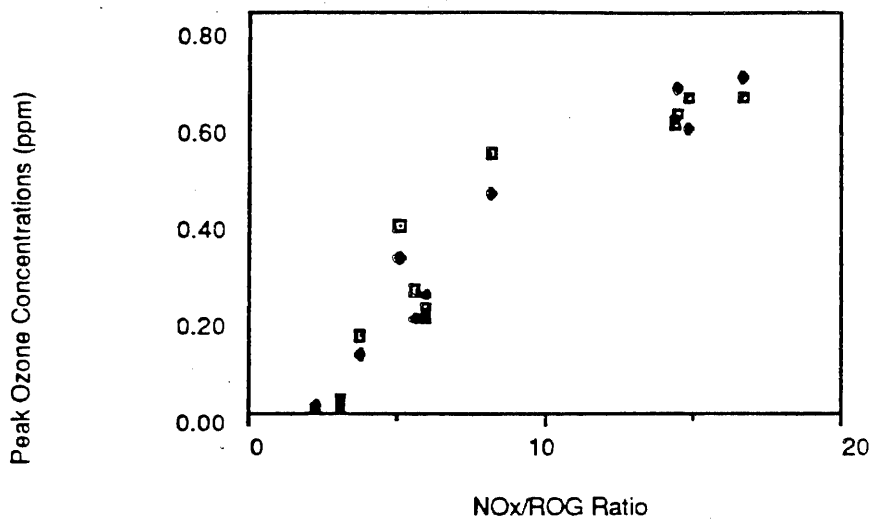


(a)

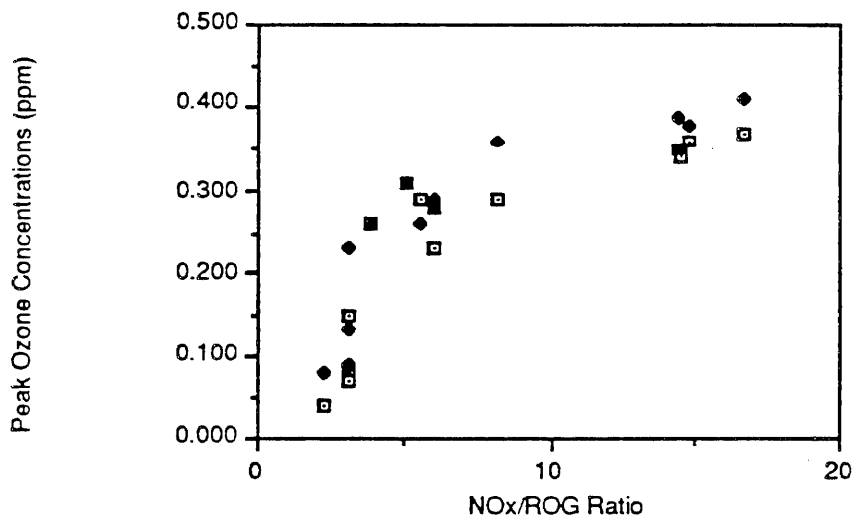


(b)

Figure 2.1 Plot of peak ozone concentrations - predicted peak ozone concentrations are plotted as a function of observed concentrations in the indoor teflon chamber. (a) Day 1 (b) Day 2



(a)

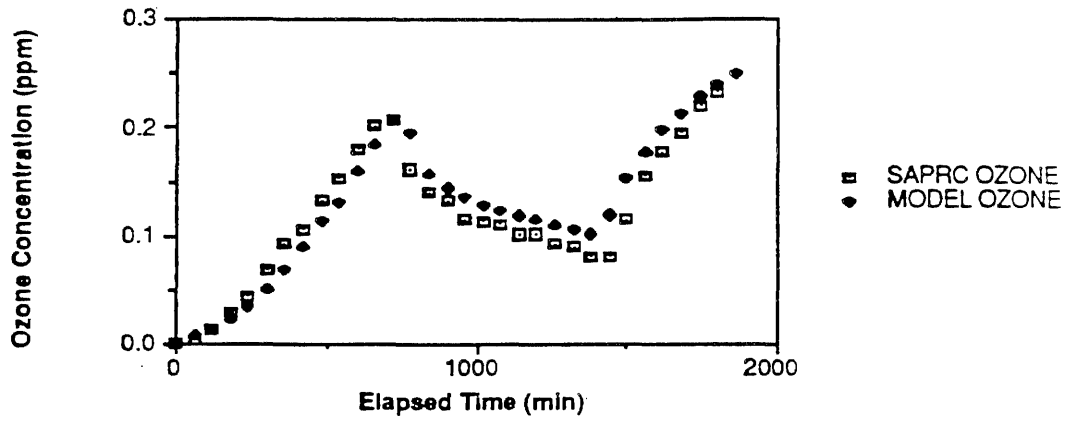


(b)

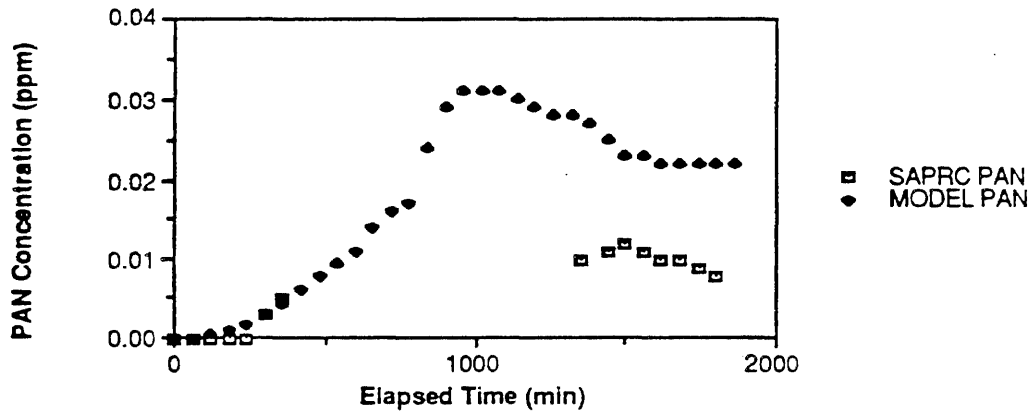
Figure 2.2 Plot of predicted, \blacklozenge , and observed, \square , ozone concentrations as a function of ROG/NOx ratio in the indoor teflon chamber. (a) Day 1 (b) Day 2

Table 2.4 Data from ITC 872

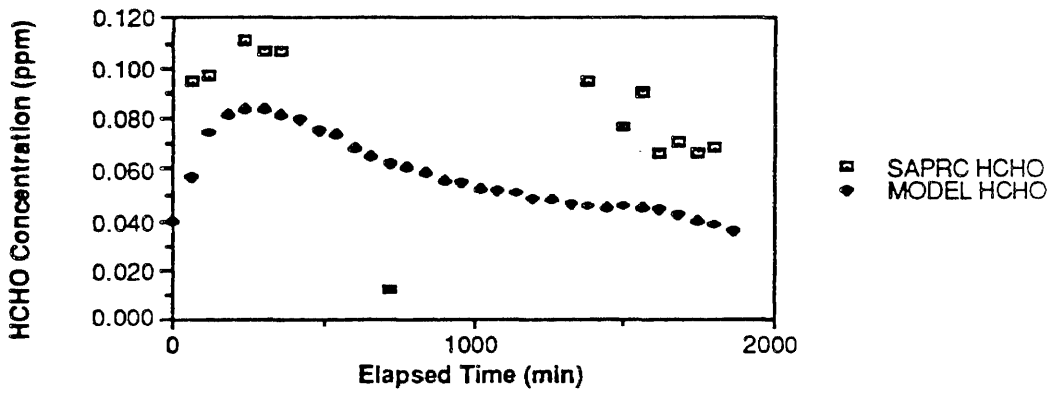
Elapsed Time (min)	SAPRC Data (ppm)			Model Data (ppm)		
	O3	PAN	HCHO	O3	PAN	HCHO
0	0.001	0		0	0	0.04
60	0.004	0	0.095	0.007	0.000086	0.057
120	0.013	0	0.097	0.014	0.00052	0.075
180	0.029	0		0.022	0.0011	0.082
240	0.044	0	0.111	0.034	0.0019	0.084
300	0.069	0.003	0.107	0.049	0.003	0.084
360	0.092	0.005	0.107	0.068	0.0043	0.082
420	0.106			0.09	0.006	0.08
480	0.131			0.112	0.0078	0.076
540	0.153			0.13	0.0093	0.074
600	0.179			0.159	0.011	0.069
660	0.201			0.183	0.014	0.066
720	0.206		0.012	0.206	0.016	0.063
780	0.161			0.195	0.017	0.061
840	0.14			0.157	0.024	0.059
900	0.132			0.143	0.029	0.056
960	0.115			0.135	0.031	0.055
1020	0.112			0.128	0.031	0.053
1080	0.111			0.122	0.031	0.052
1140	0.102			0.118	0.03	0.051
1200	0.102			0.114	0.029	0.049
1260	0.092			0.109	0.028	0.048
1320	0.089			0.105	0.028	0.047
1350		0.01				
1380	0.081		0.095	0.102	0.027	0.046
1440	0.081	0.011		0.119	0.025	0.045
1500	0.115	0.012	0.077	0.152	0.023	0.046
1560	0.154	0.011	0.091	0.176	0.023	0.045
1620	0.175	0.01	0.067	0.196	0.022	0.044
1680	0.195	0.01	0.071	0.213	0.022	0.042
1740	0.22	0.009	0.067	0.227	0.022	0.04
1800	0.232	0.008	0.069	0.239	0.022	0.038
1860				0.249	0.022	0.036



(a)



(b)



(c)

Figure 2.3 Plot of predicted, \bullet , and observed, \square , pollutant concentrations for experiment ITC 872. (a) Ozone (b) PAN (c) HCHO

2.3.2.2 OTC Test Results

Of the 42 OTC test runs, the 17 runs that involved methanol and had usable data were modeled in this study. Only tests with methanol and/or formaldehyde were investigated because the mechanism was previously tested against standard hydrocarbon mixtures. One experiment lasted one day, one for three days and the remainder for two days. A summary of the calculated and measured peak ozone concentrations and timing is given in Table 2.5.a and 2.5.b for days 1 and 2, respectively. Unfortunately, the ozone could not be measured too frequently in the OTC because that would have depleted the bag excessively over the three days. Because of this, some of the ozone peaks were missed. However, peak values can be extrapolated and they fit in well with the predictions obtained with the Extended Caltech mechanism. Figures 2.4a and 2.4b compare the SAPRC measured ozone for the OTC tests to that calculated using the Extended Caltech mechanism. Agreement is quite good. On day one only, three runs have errors exceeding 30% and six have errors smaller than 5%. On day two the agreement is even better, with only three runs having errors exceeding 30% and ten showing agreement to within 5%. The mechanism also predicted the time at which the peak would occur for both days. The accuracy of the predicted peak timing was comparable to the more detailed SAPRC explicit mechanism.

Concentrations of ozone, PAN, and formaldehyde for runs OTC 231, 237, 241 and 242 are shown in Figures 2.5, 2.6, and 2.7. As discussed previously, ozone peak concentrations match remarkably well. Ozone concentration plots vs. time for OTC runs 231, 237, 241, and 242 are shown in Figure 2.5a, b, c, and d, respectively. Agreement is noted between the predicted and observed ozone concentrations throughout the duration of the experiment. PAN concentration plots vs. time for the OTC runs are shown in Figures 2.6a, b, c, and d. PAN predictions, as expected, run consistently lower in the SAPRC measurements throughout the time plot. However, general trends in growth are also followed. HCHO concentration plots, shown in Figures 2.7a, b, c, and d, carry a large degree of error compared to ozone and PAN. This is expected, as the SAPRC data shows a significant amount of scattering in the measurements. As discussed previously, this is due to the difficulty in obtaining accurate experimental HCHO measurements.

Modeled and observed concentrations of alkanes, olefins (propane measured by SAPRC), ethene, aromatics, methanol, NO, NO₂, and isobutene were taken for OTC run 231, and are shown in Figures 2.8 and 2.9. As can be seen from these graphs, agreement is good throughout the experiment. As discussed above, SAPRC measurements for NO₂ were higher than model predictions, but this is explained by the possibility of the measuring devices experiencing interference from other oxidized nitrogen compounds. The Extended Caltech predictions are consistent with the detailed mechanism.

2.3.3 Alternative Chemical Mechanisms

Three new chemical mechanisms have been released since the beginning of this study. The first, the SAPRC/ERT mechanism (Lurmann et al. 1987) is a lumped molecule mechanism, as is the Regional Acid Deposition Model (RADM) mechanism (Stockwell, 1988). The third, the CBM IV (Gery, 1987) mechanism uses the carbon bond approach. Each have been designed for use in photochemical models, though the RADM mechanism is for regional scale simulations. The SAPRC/ERT mechanism is very well documented, and the mechanism was condensed from an explicit mechanism which was tested against multi-day smog chamber experiments, including methanol chemistry experiments. The condensed mechanism has also been evaluated against the original explicit mechanism and experiments. It is recommended that this mechanism, or another updated one, be used in

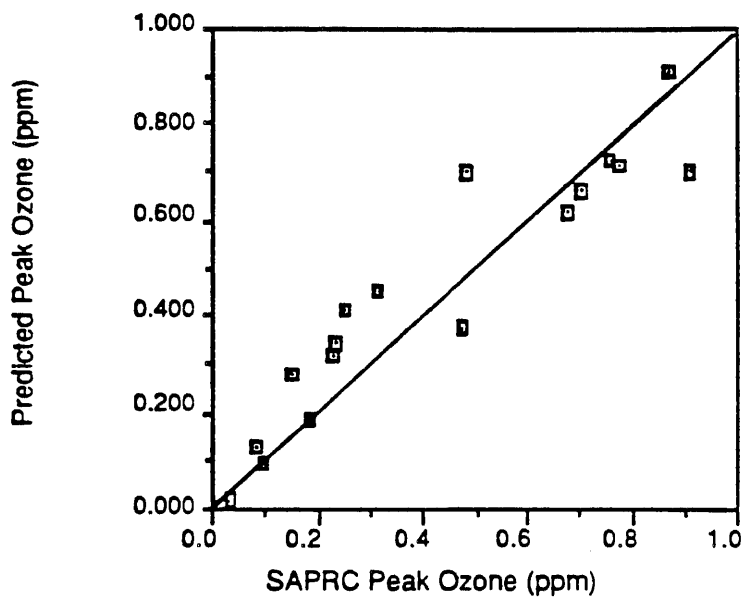
OTC Run Number	SAPRC Experimental Peak Ozone Conc.		Calculated Peak Ozone Conc.	
	(ppm)	time (hrs)	(ppm)	time (hrs)
215	.868	5.50	.913	5
217	.483	5.75	.703	5
219	.475	6.00	.377	6
221	.235	5.50	.344	6
222	.909	5.75	.698	6
224	.776	5.75	.715	6
229	.253	6.00	.417	6
231	.098	6.00	.097	6
237	.757	5.75	.727	6
238	.702	6.00	.661	6
240	.034	5.75	.019	6
241	.674	5.50	.617	6
242	.182	6.00	.184	5
243	.152	5.50	.279	6
248	.080	6.00	.130	6
249	.317	6.00	.450	6
250	.230	6.00	.320	6

(a)

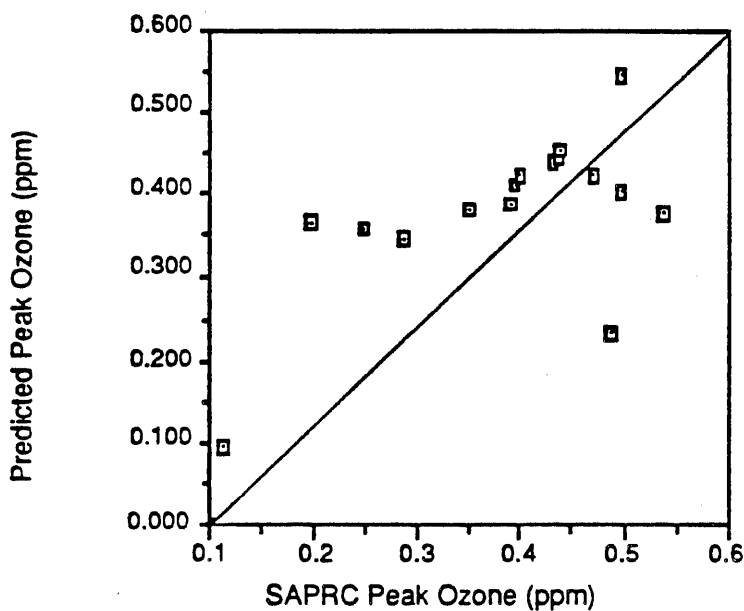
OTC Run Number	SAPRC Experimental Peak Ozone Conc.		Calculated Peak Ozone Conc.	
	(ppm)	time (hrs)	(ppm)	time (hrs)
215	.498	28	.545	27
219	.287	28	.349	30
221	.394	30	.411	30
222	.497	24	.404	24
224	.439	24	.456	24
229	.538	30	.380	30
231	.389	30	.391	30
237	.436	28	.448	29
238	.431	30	.438	29
240	.114	30	.095	30
241	.471	29	.425	29
242	.351	29	.383	30
243	.487	30	.233	30
248	.400	30	.424	29
249	.248	29	.358	30
250	.199	29	.367	30

(b)

Table 2.5 OTC Predicted and Observed Peak Ozone Concentrations
(a) Day 1 (b) Day 2

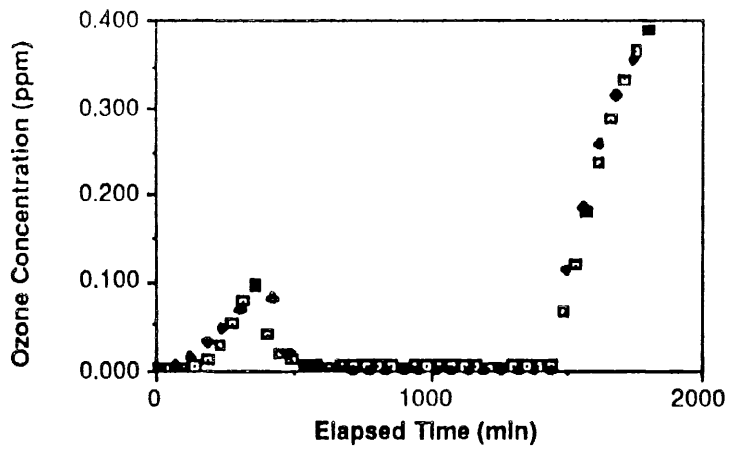


(a)

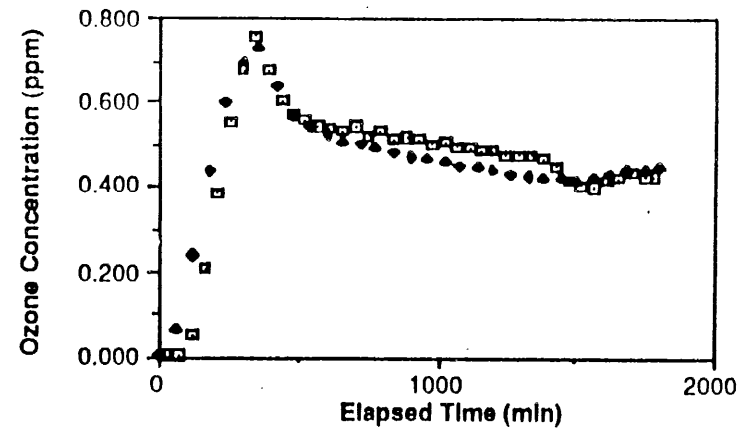


(b)

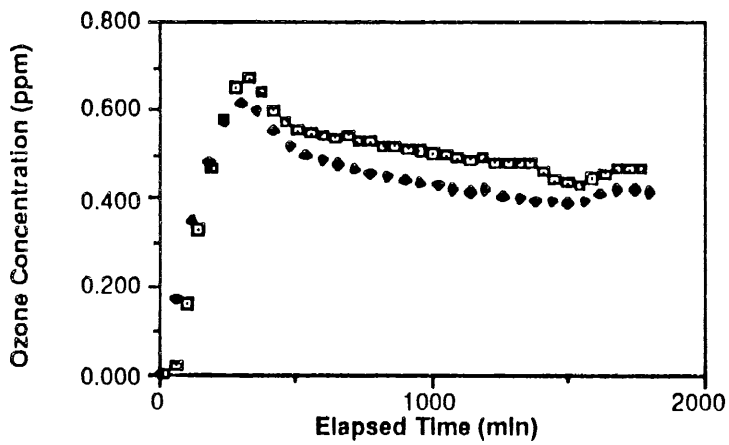
Figure 2.4 Plot of peak ozone concentrations, predicted vs. SAPRC test data (a) Day 1 (b) Day 2



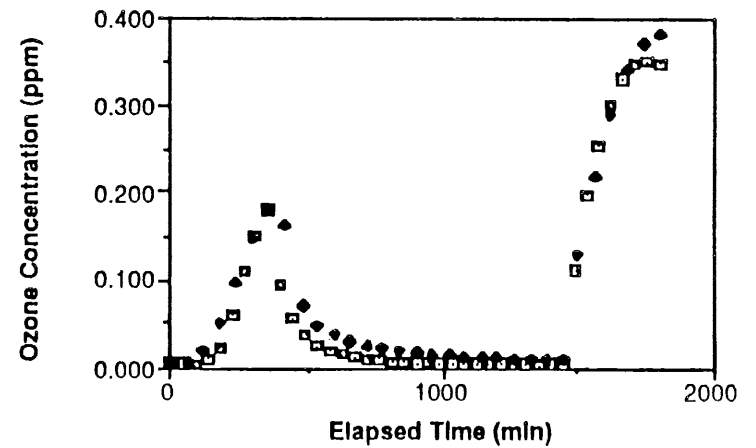
(a)



(b)



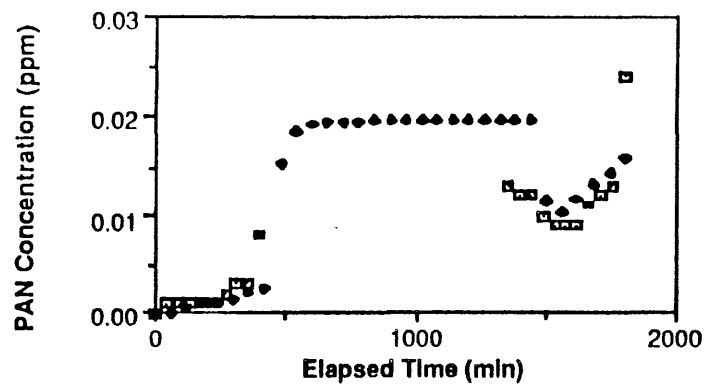
(c)



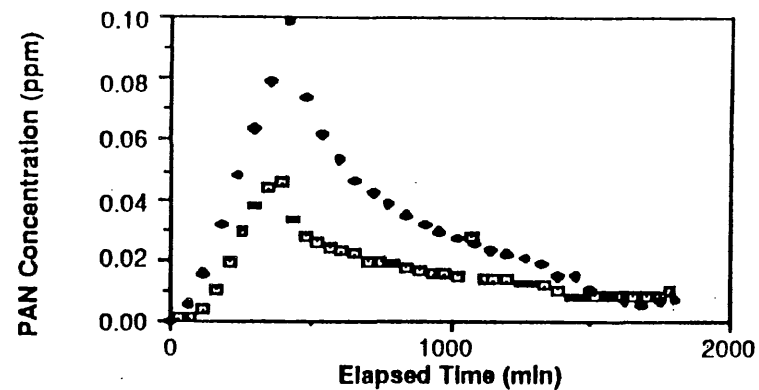
(d)

Figure 2.5 Plot of predicted, \blacklozenge , and observed, \blacksquare , ozone concentrations as a function of time for SAPRC outdoor teflon chamber experiments.

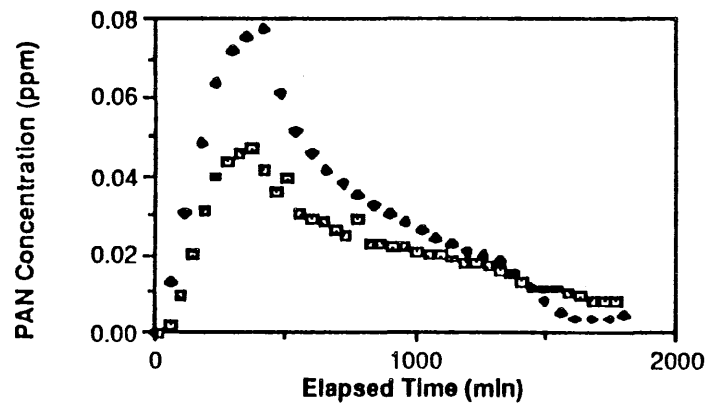
(a) OTC 231 (b) OTC 237 (c) OTC 241 (d) OTC 242



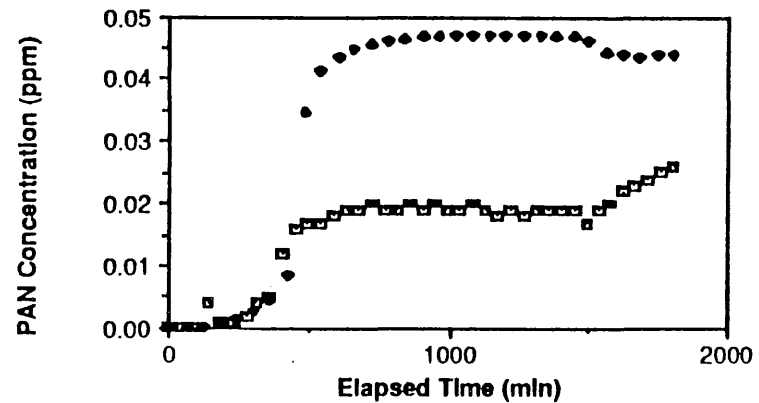
(a)



(b)



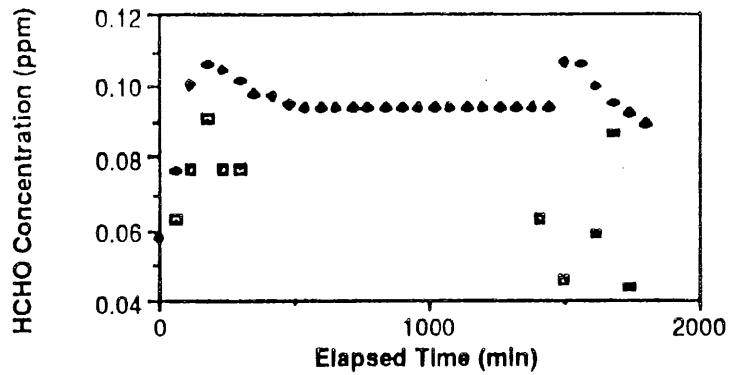
(c)



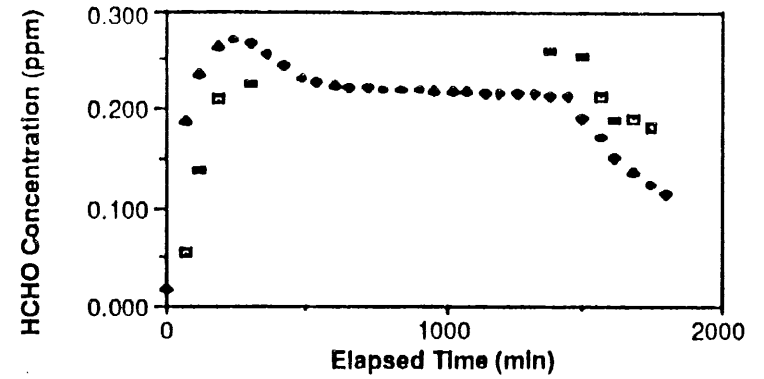
(d)

Figure 2.6 Plot of predicted, \blacklozenge , and observed, \square , PAN concentrations as a function of time for SAPRC outdoor teflon chamber experiments.

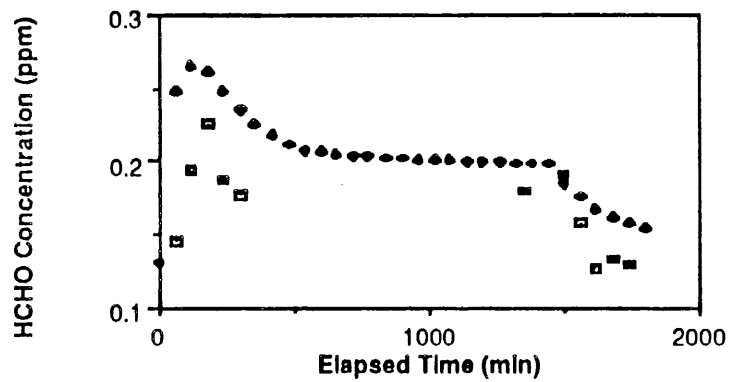
(a) OTC 231 (b) OTC 237 (c) OTC 241 (d) OTC 242



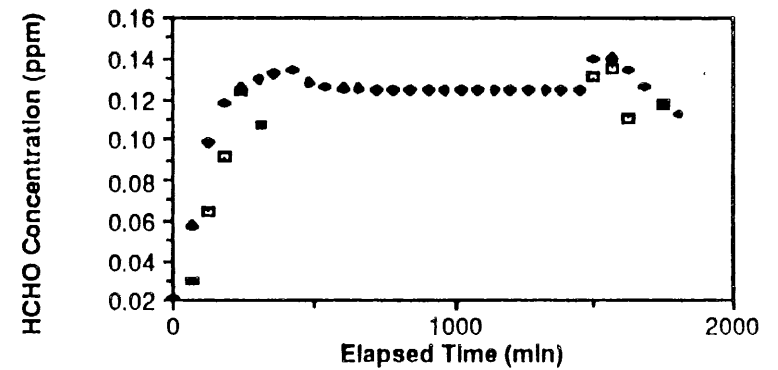
(a)



(b)

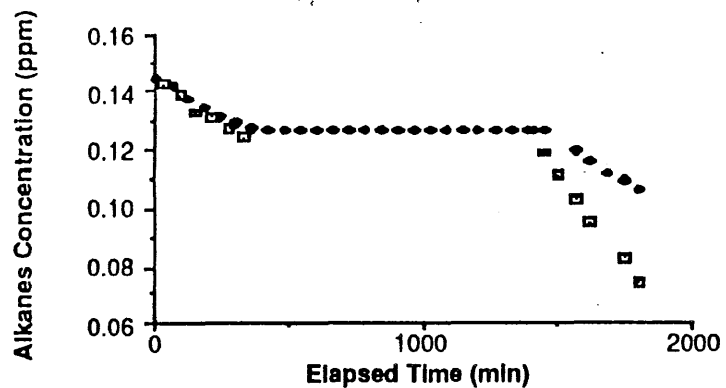


(c)

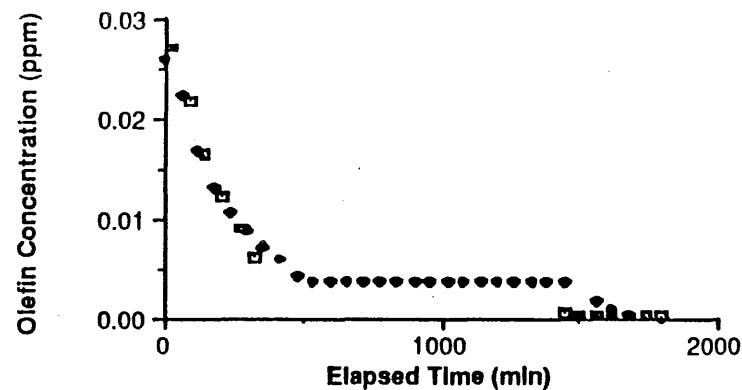


(d)

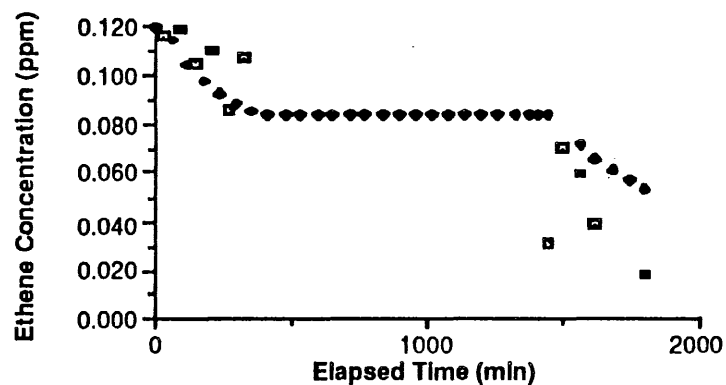
Figure 2.7 Plot of predicted, \bullet , and observed, \square , HCHO concentrations as a function of time for SAPRC outdoor teflon chamber experiments.
 (a) OTC 231 (b) OTC 237 (c) OTC 241 (d) OTC 242



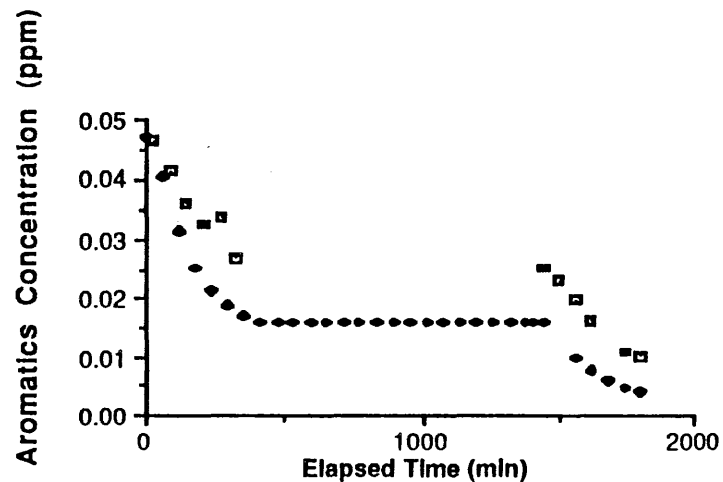
(a)



(b)

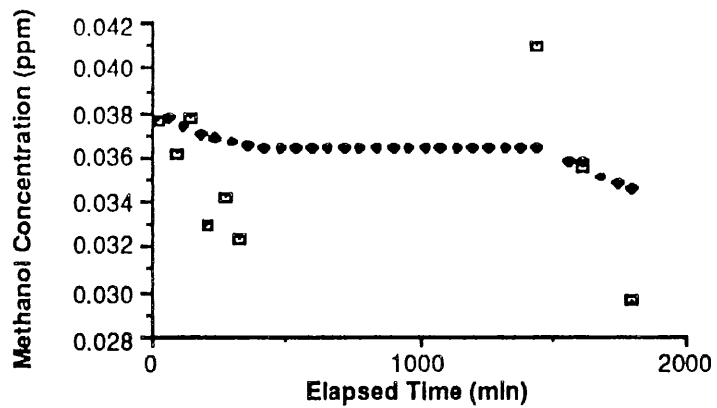


(c)

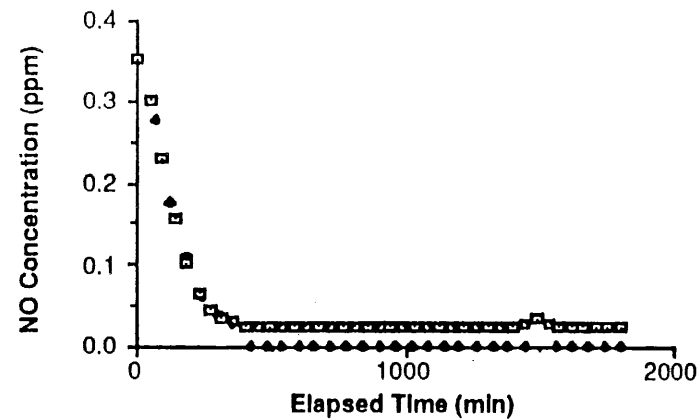


(d)

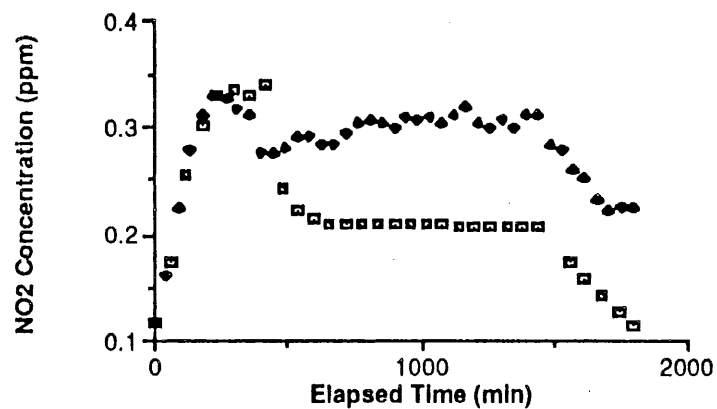
Figure 2.8 Plot of predicted, \bullet , and observed, \square , species concentration as a function of time for SAPRC OTC 231.
 (a) Alkanes (b) Olefins (c) Ethene (d) Aromatics



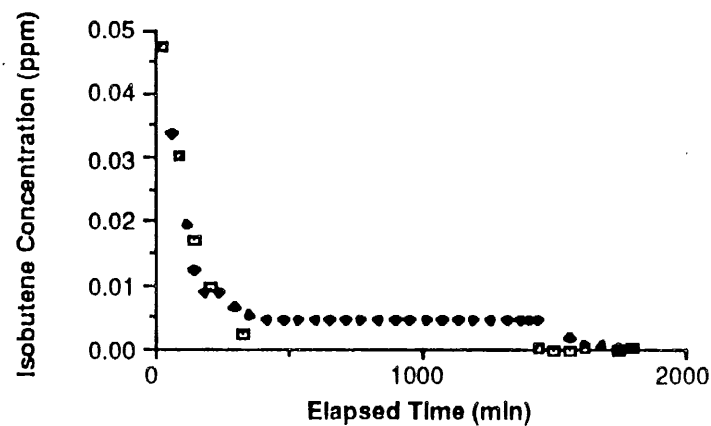
(a)



(b)



(c)



(d)

Figure 2.9 Plot of predicted, \bullet , and observed, \square , species concentration as a function of time for SAPRC OTC 231.
 (a) Methanol (b) NO (c) NO₂ (d) Isobutene

future studies. In the next chapter, the sensitivities of the Caltech mechanism are compared to similar tests of the SAPRC/ERT mechanism.

The major differences between the SAPRC/ERT mechanism and the Extended Caltech mechanism are in the number of primary organic compounds and in the number of radical-radical reactions. SAPRC/ERT has ten primary organic compounds while, excluding methanol, the Extended Caltech has six. Extension of the Caltech mechanism relied on the same database as was used to develop the SAPRC/ERT mechanism, so the rate constants and reaction products are largely similar. In a separate sensitivity analysis, Milford (1988) showed that the mechanism behave similarly under the conditions present in urban atmospheres.

2.4 Limitations of Smog Chamber Results for Evaluating Methanol Strategy Effectiveness

Results from the SAPRC experiments described and modeled here indicated that replacing one third of the base ROG mixture with methanol resulted in substantial reductions in ozone levels on the first day. However, ozone levels on the second and third days approached the values found if methanol had not been substituted. This led to concern that methanol use may not lead to an improvement in ozone air quality during multiday smog episodes. A series of model simulations were conducted to explain the results. Two types of tests were conducted. One set of tests looked at what limited ozone production on the latter days of the experiment and the other looked at the radical sources during the experiment.

It was found that on the second and third days of the simulations very little NO_x (NO and NO_2) remained. The ROG/ NO_x ratio was very high -- much higher than is found in the SoCAB. NO_x has a relatively short lifetime compared to organics like toluene, butane and octane, so by the second day most of the NO_x has reacted to form HNO_3 and PAN, and is not available to help produce O_3 . At this point ozone formation was NO_x -limited, and the reactivity of the organics had a very small effect. When NO_x was added (either in the model simulation or in the smog chamber experiments), ozone formation increased, as did sensitivity to the reactivity of the ROG. When this was done, methanol replacement led to an ozone reduction. In order to accurately assess the impact that changing the reactivity of the organics will have on ozone formation, it is necessary to continually add NO_x to keep the ROG/ NO_x levels in accord with urban conditions.

A second set of tests showed that the wall was a major source of OH radical production during the experiments. This was particularly true on the second and third days when the lack of NO to reduce HO_2 to OH became critical. Under this condition, the wall radical production can help drive the chemistry, increasing the apparent reactivity of the organics (and decreasing the NO_x , too). It is important to "back out" the effect of wall radicals by modeling the chamber conditions with and without this source.

Smog chambers cannot show the impact of atmospheric dispersion, including stratification. This can be important for simulating multiday effects. They are, instead, ideal for testing the chemical mechanisms in models that can describe pollutant evolution over multiple days under real atmospheric conditions.

2.5 Conclusions

In general, for the smog chamber experiments containing methanol and formaldehyde, the Extended Caltech mechanism was able to predict both the measured peak ozone concentrations and the timing of these peaks. The mechanism appears to perform comparably to the explicit SAPRC model for these simulations. The Extended Caltech mechanism, including chamber and experiment dependent characteristics, appears to account for the significant physical and chemical phenomena occurring inside the smog chambers.

Agreement between the model and the experiments for formaldehyde data was generally satisfactory, though the scatter in the measurements inhibited detailed analysis. The model correctly predicted overall trends in formaldehyde levels, in most cases. Likewise, agreement on PAN data was reasonable. The model consistently predicted higher PAN concentrations, as would be expected from the inclusion of PAN analogues in the mechanisms lumped species PAN. Comparisons of the other species, such as alkanes, NO_x , aromatics, and ethene was acceptable. The results indicate that the Extended Caltech mechanism is correctly tracking the evaluation of these species.

Comparison of the Extended Caltech mechanism against other, more recent mechanisms, showed that it behaved similarly at the concentrations experienced in the SoCAB. This finding is reinforced by the general agreement between the Caltech mechanism's predictions with the SAPRC explicit mechanism and experiments. In view of these findings, the Extended Caltech mechanism should be quite capable of accurately modeling atmospheric chemistry in scenarios with or without significant methanol emissions.

3.0 Sensitivity Analysis of the Chemical Mechanism and Ozone Production to Methanol and Formaldehyde

In any modeling exercise, there will be uncertainties in the predictions due to uncertainties in the inputs and model components. The three-tiered structure of the study was developed to identify the uncertainties arising from each step in modeling complexity in as great of detail as feasible. One advantage of this approach is that formal sensitivity tools can be applied to certain components of the models when it is impractical to apply those tools to the complete system. In this chapter, results are presented from applying the Direct Decoupled Method (DDM) (Dunker, 1984; McCroskey and McRae, 1985) to the Chemical Mechanism under a variety of conditions. DDM is a powerful local sensitivity uncertainty analysis procedure for elucidating how a system responds to input parameters. In the case at hand, the inputs are pollutant concentrations, emissions and reaction rates. The analysis has been used to show how ozone, formaldehyde and other pollutants respond to inputs. In conjunction with the previous chapter, this gives a detailed view of the mechanism performance.

A second object of this study is to examine, from a purely chemical standpoint, the response of an urban atmosphere to varying the composition and levels of ROG and NO_x. A particular interest in this part of the analysis is looking at the ozone formation potential of methanol and formaldehyde emissions. Note that, as also shown by Carter (1988a) and Chang (1988), this is not an absolute quantity, but depends on the ambient conditions and the levels of other pollutants.

As discussed in the previous chapter, since the beginning of this study, a new chemical mechanism, the SAPRC/ERT mechanism, has been released. It was decided to analyze both that mechanism and the Caltech mechanism under similar conditions. A more detailed sensitivity analysis of both the Caltech and ERT/SAPRC mechanism, as well as the Regional Acid Deposition Model (RADM) chemical mechanism and the Carbon Bond IV (CBM IV) mechanism can be found in Milford (1988). The results of Milford and co-workers will be discussed in context with this study's findings.

3.1 Simulation and Sensitivity Analysis Methods and Conditions

Both the Caltech and SAPRC/ERT mechanisms were analyzed simulating three levels of methanol fuel use. Unlike the smog chamber simulations in the previous chapter, these calculations included continuous emission of ROG and NO_x. This is to more closely represent ambient conditions. The two mechanisms are briefly described below, followed by a description of the modeling conditions.

3.1.1 The Caltech Mechanism

As presented in the Chapter 2, the Caltech mechanism has been modified from the mechanism presented in Russell, et al. (1988), which in turn is an update of McRae, et al. (1982). The rate constants for some reactions have been updated for this analysis based on the work of Carter, et al. (1986ab). The mechanism uses 30 species in 57 reactions, including the CH₄O - OH reaction (Carter et al., 1986a). Rate constants for reactions involving each stable organic class are determined explicitly for a given initial ROG composition as the mole-weighted sum of the rate constants of each of the individual organic species present. The mechanism includes two primary carbonyl classes, ethylene and one higher olefins class, one class of alkanes, and one class of aromatics. A comparison of the Caltech mechanism with smog chamber results has been presented in McRae (1982).

3.1.2 The SAPRC/ERT Mechanism

The SAPRC/ERT mechanism used here is the "ERT/SAPRC OZIPM" mechanism presented in Lurmann, et al. (1987), and was obtained from that document. The mechanism was condensed from a more detailed mechanism which was developed from the mechanism of Atkinson, et al. (1982), and the review of Carter, et al. (1986). The ERT mechanism contains 131 reactions and 50 species. The reaction of methanol with hydroxyl radical:



was added for this analysis. Groups of individual stable organic species with similar reaction rates and yields are represented by surrogate species, for which reaction rate constants and product yields have been pre-set based on an assumed mixture. Four primary carbonyl classes, two alkane classes, ethylene, two classes of higher olefins, and three aromatics classes are included. The detailed version of the SAPRC/ERT mechanism has been tested extensively against smog chamber results from the California State Air Pollution Research Center (SAPRC) and UNC chambers. The version included in this analysis was tested by comparison against the detailed mechanism (Lurmann, et al., 1987).

3.1.3 Simulation Conditions

The kinetic simulations and sensitivity analysis were run over a 36-hour period simulating two days and one night. Photolytic rates were varied diurnally as calculated for Los Angeles on September 1, based on the zenith angle-dependent rates given in Lurmann, et al. (1987). A constant temperature of 298 K and relative humidity of 50 percent were maintained throughout the simulations. No dilution or smog chamber-dependent reactions were included.

The initial conditions used for 1) the base case, 2) 50 and 3) 100 percent displacement cases are listed for each mechanism in Table 1. Emissions were input at a constant rate over the 36-hour period, in the same proportions as the initial conditions. The emissions rates were set so that over 36 hours, the integrated flux of each species was equal to three times the initial concentrations. Total inputs of NO_x and ROG in the base case were thus 0.4 ppm and 4.0 ppmV, of which one fourth was the initial concentration and three-fourths were input as emissions. The non-methanol ROG input was reduced as explained below for the 50 and 100 percent methanol substitution cases. The NO_x input was constant across the three cases. The ROG composition used with both the SAPRC/ERT and Caltech mechanisms is based on a typical morning mixture for an urban area, derived from the average morning ROG compositions reported in Grosjean and Fung (1984) and in Bauges (1986). Grosjean and Fung's data are the average of measurements made over 23 days during the Fall of 1981 at a downtown Los Angeles location. The data reported in Bauges are the average of the median morning compositions reported for the 1984 and 1985 summer season in approximately 20 cities. The ROG composition was translated for input into each mechanism as recommended in the available documentation.

Table 3.1. Initial Concentrations (ppmV) Used in Kinetic Simulations and Sensitivity Analysis.

	Caltech Mechanism		
	Case 1 Base	Methanol Substitution	
		Case 2 50%	Case 3 100%
NO ₂	0.025	0.025	0.025
NO	0.075	0.075	0.075
CO	1.0	1.0	1.0
HCHO	0.035	0.030	0.026
RCHO	0.029	0.023	0.018
C ₂ H ₄	0.017	0.013	0.010
OLE	0.028	0.022	0.017
ALK	0.139	0.111	0.083
CH ₄ O	0.000	0.039	0.077
ARO	0.041	0.038	0.029

	SAPRC/ERT Mechanism		
	Case 1 Base	Methanol Substitution	
		Case 2 50%	Case 3 100%
NO ₂	0.025	0.025	0.025
NO	0.075	0.075	0.075
CO	1.0	1.0	1.0
HCHO	0.035	0.030	0.026
ALD ₂	0.017	0.014	0.010
RCHO	0.012	0.0096	0.0072
ALK ₄	0.077	0.062	0.046
ALK ₇	0.034	0.032	0.024
ETHE	0.017	0.013	0.0099
PRPE	0.015	0.012	0.0088
TBUT	0.014	0.011	0.0081
TOLU	0.016	0.013	0.0096
XYLE	0.018	0.014	0.011
CH ₄ O	0.000	0.039	0.077

For the 50 and 100 percent displacement cases, the methanol fraction and reduced ROG fractions were derived as follows. Mobile source emissions were assumed to comprise 40 percent of the current (prior to fuel substitution) area-wide ROG emissions. Alkanes and other organics were reduced 20% (for the 50% displacement case) to 40% (for 100% displacement). CH₄O and formaldehyde were then increased to simulate MFV usage. Formaldehyde emissions from methanol-fueled vehicles were assumed to be 5 percent of the CH₄O emissions, on a carbon basis. Assuming proportionality between ROG emissions and ambient concentrations, and assuming there is no change in the number of vehicle-miles traveled, the ratio of the initial methanol concentration to its emission rate is equal to the ratio of the current fraction of the initial alkane concentration attributed to mobile sources to the alkane emissions rate. The resulting initial methanol concentration is 0.0385 ppmV with 50 percent displacement, and 0.077 ppmV with 100 percent displacement. Again, the emissions rate was set so that the integrated flux of CH₄O over 36 hours would equal three times the initial concentration.

3.1.4 Sensitivity Analysis Methodology

The Direct Decoupled Method (Dunker, 1984; McCroskey and McRae, 1985) is a local sensitivity analysis technique which gives the time-dependent sensitivities of the output species to the initial conditions and reaction and emissions rate constants in the system. The concentrations output from chemical kinetic simulations are numerical approximations to the solution of the system of equations:

$$u' - f(u,t;p) = 0, \quad (3.2)$$

$$u(t_0) = u_0.$$

u = the vector of concentrations;

u_0 = the vector of concentrations at $t = 0$; and

$$u' = \frac{d u}{d t}.$$

With p representing both rate constants and initial concentrations, the first order sensitivity coefficients with respect to p are the solutions to:

$$s' - \left(\frac{d f}{d u} s + \frac{d f}{d p} \right) = 0, \quad (3.3)$$

$$s(t_0) = \frac{d u_0}{d p}$$

$$s = \frac{d u}{d p} \text{ and}$$

$$s' = \frac{ds}{dt}$$

As implemented, the Direct Decoupled Method differentiates the numerical approximation to the set of equations (3.2) with respect to p , and solves concurrently for the concentrations and sensitivity coefficients using the Gear algorithm.

The sensitivity measure presented in this analysis is the time-integrated, normalized coefficient:

$$S_i(t) = \int_0^t \frac{p_i \partial[\text{O}_3(t)]}{\partial p_i} \text{ (ppm) } , \quad (3.4)$$

where $[\text{O}_3(t)]$ is the time-varying concentration of O_3 , and $[p_i]$ is either the initial concentration of species i , the emission rate of species i , or the rate constant of reaction i . The normalized coefficient indicates the absolute change in the O_3 concentration (in ppm) at time t which would result from a small fractional change in p_i about its nominal value, with all other parameters held at their nominal values. Multiplying the sensitivity coefficients by the initial concentrations of rate constant values provides a measure that is comparable across parameters and hence indicates the relative importance of each.

3.2 Simulation and Sensitivity Analysis Results

The ozone concentrations predicted for the cases (1) no displacement, (2) 50 percent displacement of gasoline with methanol and (3) 100 percent displacement of gasoline with methanol are shown in Figure 3.1. The O_3 concentrations at 12, 24 and 36 hours are given in Table 3.2. Both the SAPRC/ERT and Caltech mechanisms predict that ozone concentrations decrease monotonically with the degree of methanol use. Both mechanisms further indicate that the fuel substitution is markedly less effective in reducing O_3 concentrations on the second day (the final 12 hours) of the simulations than on the first day. This result is due to the depletion of NO_x relative to ROG, which occurs over the course of the simulation as nitric acid is produced. Ozone production on the second day is thus NO_x -limited, and correspondingly relatively insensitive to the ROG input.

Table 3.2. Ozone Concentrations (ppm) Predicted for Three Levels of Methanol Substitution.

	Caltech			SAPRC/ERT		
	12 hr	24 hr	36 hr	12 hr	24 hr	36 hr
Case 1	0.460	0.284	0.680	0.436	0.256	0.539
Case 2	0.373	0.198	0.650	0.383	0.212	0.529
Case 3	0.256	0.083	0.613	0.264	0.100	0.504

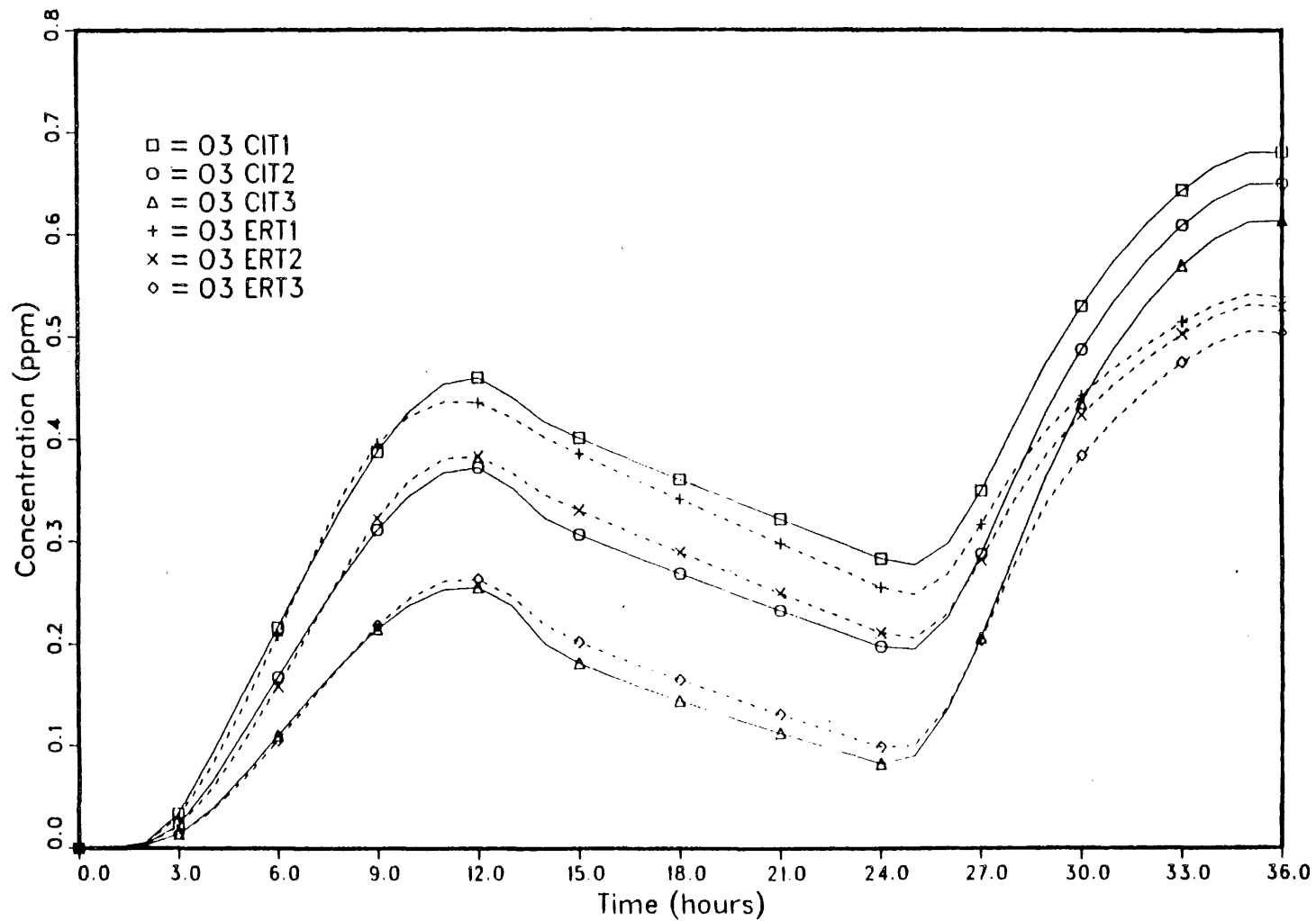


Figure 3.1 Predicted ozone using the Caltech (CIT) and SAPRC/ERT (ERT) mechanisms for the Base Case (CIT1 and ERT1), 50% methanol utilization (CIT2 and ERT2), 100% methanol utilization (CIT3 and ERT3).

The absolute predictions of the mechanisms agree to within about 0.04 ppm throughout the first 24 hours. During the second day, the concentrations predicted with the Caltech mechanism build up more than those predicted with the SAPRC/ERT mechanism. The final difference in the O₃ concentrations predicted by the two mechanisms is about 0.15 ppm. Enhanced O₃ production with the Caltech mechanism on the second day results from relatively high PAN production through the night. PAN concentrations build up because radical - radical reactions which would consume acylperoxy-radicals are not included in the original Caltech mechanism. Thermal decomposition of PAN then contributes extra NO_x to the system during the second day. This was corrected as part of the analysis in the previous chapter, and the day 2 results in the extended mechanism agree much more closely.

The effect of methanol fuel substitution on ozone is generally predicted to be slightly greater with the Caltech mechanism than the SAPRC/ERT mechanism. With the Caltech mechanism, the reduction in the peak O₃ concentration on the first day is predicted to be 0.09 ppm with a 50 percent displacement, and 0.20 ppm with a 100 percent displacement. With the SAPRC/ERT mechanism, the corresponding reductions are 0.06 and 0.18 ppm. After 36 hours, the corresponding reductions are 0.03 and 0.07 ppm with Caltech, and 0.01 and 0.04 ppm with SAPRC/ERT. These differences are explained by the respective inherent reactivities of the two mechanisms: for the initial conditions used in this analysis, the SAPRC/ERT mechanism produces more peroxy radicals, and hence is less sensitive than the Caltech mechanism to changes in the ROG input.

In addition to ozone, formaldehyde, PAN (peroxyacetyl nitrate) and nitric acid are of interest due to associated potential health or environmental damages. The concentrations of these species at the end of the first and second days in the simulations are given in Table 3, for each of the methanol substitution cases. The formaldehyde and PAN concentrations decrease monotonically as the displacement of gasoline with methanol increases. Nitric acid concentrations after 12 hours increase with the 50 percent displacement step and then decrease from that level with the additional 50 percent displacement. After 36 hours, the predicted HNO₃ concentrations consistently increase as the methanol fraction increases.

Table 3.3. Concentrations of HCHO, PAN and HNO₃ for Three Levels of Methanol Substitution.

	Caltech			SAPRC/ERT		
	At 12 Hours					
	HCHO	PAN	HNO ₃	HCHO	PAN	HNO ₃
Case 1	0.0540	0.0796	0.0731	0.0439	0.0643	0.0801
Case 2	0.0479	0.0567	0.0736	0.0413	0.0482	0.0898
Case 3	0.0395	0.0314	0.0675	0.0373	0.0263	0.0889
	At 36 Hours					
Case 1	0.0749	0.203	0.181	0.0552	0.109	0.207
Case 2	0.0682	0.175	0.207	0.0488	0.0958	0.226
Case 3	0.0592	0.139	0.240	0.0430	0.0782	0.252

3.3 Ozone Sensitivity to Initial Conditions and Emissions

Ozone formation sensitivity to initial conditions and emissions is shown in Figures 3.2 and 3.3. The integrated local sensitivity of O₃ to the initial concentration of each ROG species is shown in Figure 3.2, for both mechanisms and for the cases of no-displacement of gasoline by methanol (Figures 3.2a and 3.2b) and 100 percent displacement (Figures 3.2c and 3.2d). The sensitivity results for the 50 percent displacement case were similar to those for the 100 percent displacement case, and are not shown. The sensitivity coefficients are interpreted as follows, using the sensitivity of O₃ to the olefins class (OLE) in Figure 3.2a as an example: a small increase (e.g., a few percent) in the initial concentration of olefins over its nominal value would result in O₃ concentrations which were higher than the nominal predictions up until about 33 hours of simulation time had elapsed, and reduced concentrations for the final three hours. The largest difference would arise after 12 hours, at which point a 10 percent change in the initial olefins concentration is predicted to yield approximately a 0.004 ppm change in the O₃ concentration. The slope of the curve indicates the instantaneous effect: up until 12 hours have elapsed an increase in the initial olefins concentration would be increasing O₃ production or decreasing its consumption, beyond that point the instantaneous effect is the

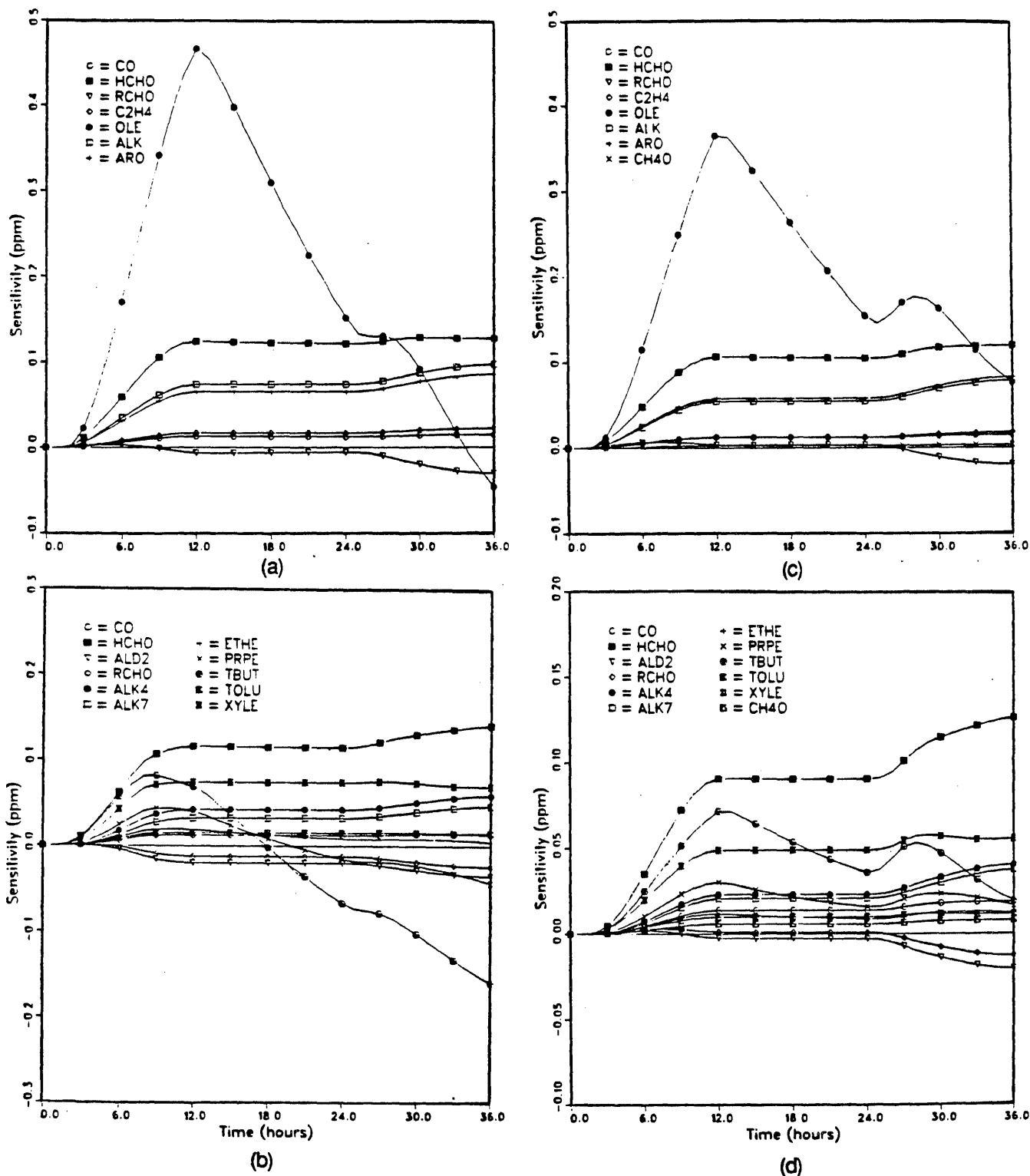


Figure 3.2 Semi-normalized sensitivity $\left(P_i \frac{\partial [O_3]}{\partial [P_i]} \right)$ of ozone formation to initial conditions

- (a) Base Case, Caltech mechanism
- (b) Base Case, SAPRC/ERT mechanism
- (c) 100% methanol utilization, Caltech mechanism
- (d) 100% methanol utilization, SAPRC/ERT mechanism.

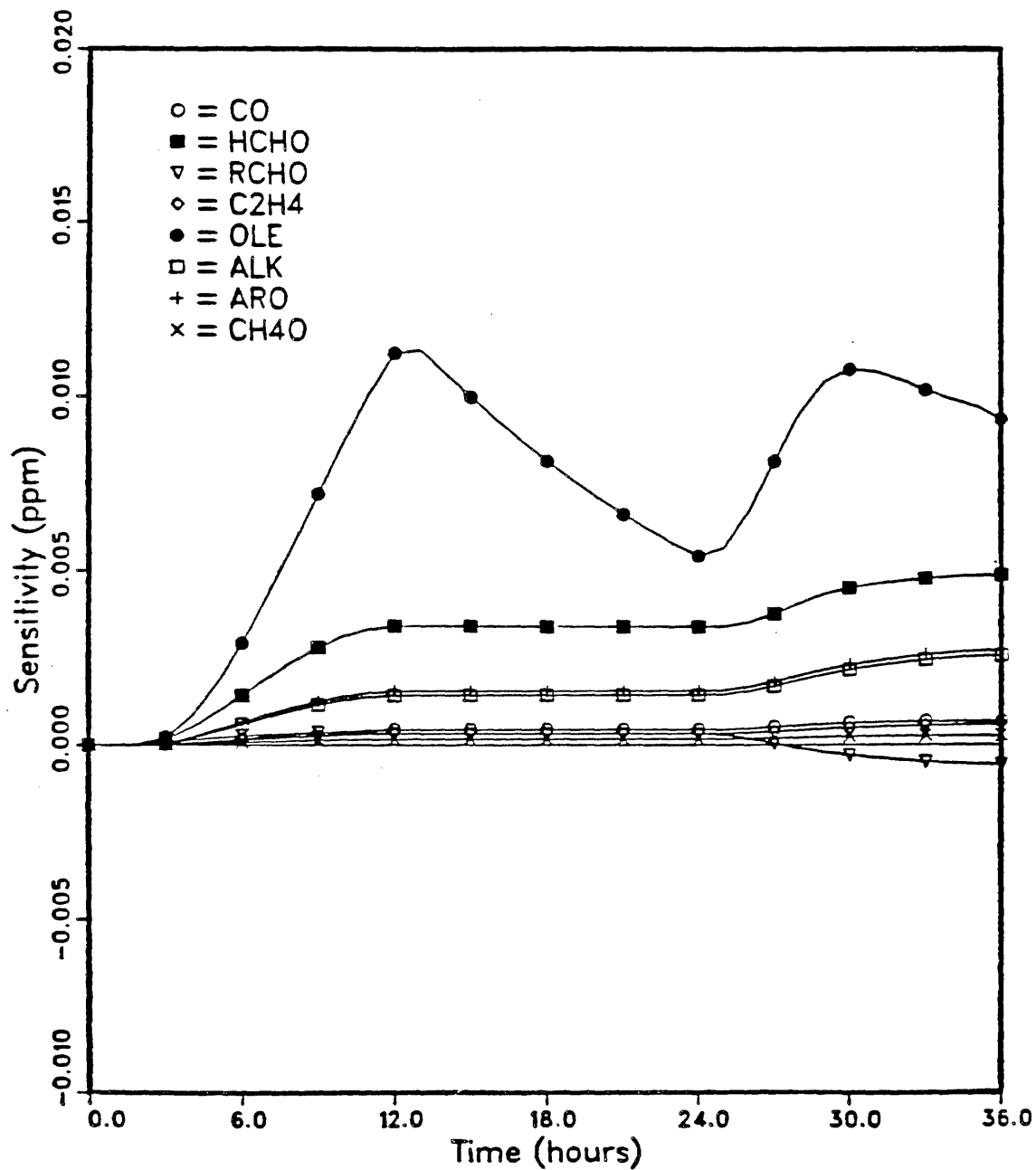


Figure 3.3. Semi-normalized sensitivity $\left(P_i \frac{\partial [O_3]}{\partial [P_i]} \right)$ of ozone formation to source emissions of various reactive organic gases and CO, corresponding to 100% methanol utilization using the Caltech mechanism.

opposite. During periods over which the sensitivity curves are flat, for example in Figure 3.2a the period from 12 to 24 hours for the sensitivity to HCHO, the initial concentration is not significantly effecting the O₃ concentration.

For case 1 conditions, the initial formaldehyde and olefin (OLE in the Caltech mechanism, and TBUT+PRPE in the SAPRC/ERT mechanism) concentrations contribute most to ozone formation during the first day (Figs 3.2a and 3.2b). On the second day, initial formaldehyde has the greatest impact of any of the ROGs. The sensitivity to HCHO is nearly the same in both simulations.

Figures 3.2c and 3.2d show the sensitivities for Case 3 simulating 100% penetration of MFVs. Initial CH₄O levels have virtually no impact on the ozone formed when compared to any of the other reactive organics in both the SAPRC/ERT and Caltech mechanism simulations (Figs 3.2 c and 3.2 d). The sensitivity of O₃ to CH₄O itself is negligible. Formaldehyde, on the other hand, is very important. If HCHO levels were greatly increased by methanol use, this would decrease the benefits of the lower reactivity of the methanol. (As discussed in Chapters 5 and 6, this is not expected to be the case.) The sensitivities of ozone formation to initial HCHO and CH₄O levels are nearly the same whether the SAPRC/ERT or Caltech mechanism is used (Fig 3.2abcd). In both simulations, the differences between Cases 1 and 3 result from reductions in the initial concentrations of the other ROG and the consequent increase in the demand for reactive organic gases. The magnitude of all of the sensitivity coefficients is lower over the first 24 hours of the simulations in Case 3 than in Case 1. This apparent effect is due to the use of normalized sensitivity coefficients. More extensive comparison and sensitivity analysis of the two mechanisms is contained in Milford (1988). That study showed that the two mechanisms performed comparably over a range of conditions.

The higher sensitivity of O₃ to olefins with the Caltech mechanism than with the SAPRC/ERT mechanism corresponds to several factors. Overall, in the nominal case, the SAPRC/ERT mechanism apparently produces more peroxy radicals for the given initial conditions than the Caltech mechanism. Thus, the sensitivity of O₃ to peroxy radical production is expected to be higher with the Caltech mechanism. Moreover, the olefins rate constants and stoichiometric coefficients used in the Caltech mechanism are weighted arithmetically based on the molar composition of the initial conditions. For the case simulated the initial ROG mixture was fairly rich in higher olefins, with the result that both the rate constants and radical production stoichiometry associated with the Caltech olefins reactions are biased on the high side. Finally, the Caltech OLE class corresponds to more than one SAPRC/ERT classes.

Figure 3.3 shows the sensitivity of ozone formation to emission source rates of the ROGs and CO. Ozone is most sensitive, on the normalized scale, to olefin emissions followed by HCHO. This is a direct reflection of the reactivity of the species. The sensitivity to CH₄O emissions is nearly zero, indicating that even after 36 hours of simulation, methanol buildup adds insignificantly to the formation of ozone.

3.4 Summary of Sensitivity Analysis

Formal sensitivity analysis of the Caltech and SAPRC/ERT mechanisms showed that methanol emissions contribute little to ozone formation over multiple day periods. The Direct Decoupled Method showed that other reactive organics, due to their higher reactivity, were responsible for most of the ozone formed.

Formal analysis of the two mechanisms showed that they behave comparably, and have similar sensitivity to methanol and formaldehyde. Ozone predictions of the two mechanisms also agreed. The similar response and sensitivities of the two mechanisms is further indication, along with the results from Chapter 2, that the extended Caltech mechanism is suitable for testing the efficacy of methanol fuel use.

This analysis indicated that formaldehyde emissions are particularly prone to forming ozone. Control of formaldehyde emissions will be critical to achieving the potential benefits of methanol utilization. This issue will be further addressed using the trajectory and airshed models.